CATHODIC PROTECTION EVALUATION

Final Report

ODOT CONTRACT PSK28885

CATHODIC PROTECTION EVALUATION

Final Report

ODOT Contract PSK28885

by

John S. Tinnea
Ryan J. Tinnea
Tinnea & Associates, LLC
2018 E. Union Street
Seattle, WA 98122-2836

for

Oregon Department of Transportation
Bridge Preservation Unit
4040 Fairview Industrial Drive SE, MS 4
Salem OR 97302-1142

October 2014

1. Report No.	2. Government Accession No.	3. Recipient's Catalog No.
4. Title and Subtitle Cathodic Protection Evaluation		5. Report Date October 2014 6. Performing Organization Code
7. Author(s) John S. Tinnea, Ryan J. Tinnea, Carmen Andrade		8. Performing Organization Report No.
9. Performing Organization Name and Address Tinnea & Associates, LLC 2018 E. Union Street Seattle, WA 98122-2836		10. Work Unit No. (TRAIS) 11. Contract or Grant No. PSK28885
12. Sponsoring Agency Name and Address Oregon Department of Transportation Bridge Preservation Unit 4040 Fairview Industrial Drive SE, MS 4 Salem, Oregon 97302-1142		13. Type of Report and Period Covered Draft Final Report 14. Sponsoring Agency Code
15. Supplementary Notes		

16. Abstract

This research investigates the effectiveness of a new corrosion rate test instrument in making field evaluations of the corrosion condition of several conventionally reinforced concrete coastal bridges. The instrument is the Gecor 9 Corrosion Rate Meter and comes with several sensors. This device is able to perform several techniques to evaluate the corrosion activity of steel reinforcement under diverse conditions. The Gecor's Sensor A is equipped with three reference electrodes (RE), 1 counter electrode (CE), and 1 guard electrode (GE). Sensor A was used to measure the rebar corrosion current, i_{corr}, using a DC galvanostatic pulse with modulated applied current confinement. This procedure was used to obtain baseline data for 21 zones of an impressed current cathodic protection (ICCP) system recently installed on the Conde McCullough Bridge in Coos Bay. That same procedure was also used to evaluate the reinforcement corrosion activity at two failed ICCP zones at the Yaquina Bay Bridge. Both of those ICCP systems utilized thermally sprayed zinc as distributed anodes. Sensor A is also able to perform an AC-based test to qualitatively evaluate the effectiveness of cathodic protection (CP) systems without the need to interrupt the applied CP current. That test protocol was applied to the same 21 ICCP zones at the Coos Bay Bridge and to six test location of the Lint Creek Bridge that has a galvanic anode CP (GACP) system installed to control rebar corrosion. Gecor Sensor B is equipped with one RE and one CE and is used to concurrently measure a rebar's corrosion potential, E_{corr}, and the resistivity of the surrounding concrete. Firmware in the Gecor 9 uses the observed corrosion potential and concrete resistivity to state the corrosion risk for the steel at the location tested. In general, the Gecor 9 performed very well. However, although it is a sophisticated instrument, it is able to produce data that is clearly questionable. Fortunately, since the Gecor has the ability to perform several markedly different types of tests, inconsistencies are generally obvious and a suspicious reading can be re-tested. Measurement errors were less a problem on the Yaquina Bay and Lint Creek Bridges because rebar could be clearly located before testing. At Coos Bay, the presence of a new zinc coating interfered with being able to identify rebar locations prior to removing the zinc on the concrete surface. At locations where reference electrodes were present and in areas of rebar structure bonds, a reasonable estimation of the rebar location could be made prior to removal of the zinc anode over an area of 8-9 inches in diameter to allow testing with the Gecor. Generally speaking, the Gecor 9 was able to make reasonable evaluations of cathodically protected rebar without having to interrupt the CP system. In terms of CP operation, this research demonstrated that: 1) the GACP system at Lint Creek is working well and protecting the embedded rebar; 2) All 12 locations tested in the two failed CP zones at Yaquina Bay reflect passive behavior of the embedded rebar even after the CP current had been interrupted for a number of years; Although the Gecor performance at Coos Bay was not as consistent as observed at the other bridges, it appears for future application, if rebars at test locations were located prior to applying the zinc coating, the test could be conducted with the sensor in proper alignment with the embedded steel, and that would significantly improve the performance of the instrument.

17. Key Words	18. Distribution Statement
bridge preservation, cathodic protection, corrosion rate testing, discrete anodes, electrochemical impedance, linear polarization, reinforced concrete, thermal sprayed zinc	

19. Security Classification (of this report)	20. Security Classification (of this page)	21. No. of Pages	22. Price
Unclassified	Unclassified	Report 81 - Appendices 133	

Technical Report Form DOT F 1700.7 (8-72) Reproduction of completed page authorized

SI* (MODERN METRIC) CONVERSION FACTORS

APPROXIMATE CONVERSIONS TO SI UNITS

Symbol	When You Know	Multiply By	To Find	Symbol
		LENGTH		
in	inches	25.4	millimeters	mm
ft	feet	0.305	meters	m
yd	yards	0.914	meters	m
mi	miles	1.61	kilometers	km
		AREA		
in^2	square inches	645.2	millimeters squared	mm^2
ft^2	square feet	0.093	meters squared	m^2
yd^2	square yards	0.836	meters squared	m^2
ac	acres	0.405	hectares	ha
mi^2	square miles	2.59	kilometers squared	km^2
		VOLUME		
fl oz	fluid ounces	29.57	milliliters	mL
gal	gallons	3.785	liters	L
ft^3	cubic feet	0.028	meters cubed	m^3
yd^3	cubic yards	0.765	meters cubed	m^3
NOTE: Volumes greater than 1000 L shall be shown in m^3.				
		MASS		
oz	ounces	28.35	grams	g
lb	pounds	0.454	kilograms	kg
T	short tons (2000 lb)	0.907	megagrams	Mg
		TEMPERATURE (exact)		
°F	Fahrenheit temperature	5(F-32)/9	Celsius temperature	°C

APPROXIMATE CONVERSIONS FROM SI UNITS

Symbol	When You Know	Multiply By	To Find	Symbol
		LENGTH		
mm	millimeters	0.039	inches	in
m	meters	3.28	feet	ft
m	meters	1.09	yards	yd
km	kilometers	0.621	miles	mi
		AREA		
mm^2	millimeters squared	0.0016	square inches	in^2
m^2	meters squared	10.764	square feet	ft^2
ha	hectares	2.47	acres	ac
km^2	kilometers squared	0.386	square miles	mi^2
		VOLUME		
mL	milliliters	0.034	fluid ounces	fl oz
L	liters	0.264	gallons	gal
m^3	meters cubed	35.315	cubic feet	ft^3
m^3	meters cubed	1.308	cubic yards	yd^3
		MASS		
g	grams	0.035	ounces	oz
kg	kilograms	2.205	pounds	lb
Mg	megagrams	1.102	short tons (2000 lb)	T
		TEMPERATURE (exact)		
°C	Celsius temperature	1.8 + 32	Fahrenheit	°F

* SI is the symbol for the International System of Measurement (4-7-94 jbp)

ACKNOWLEDGEMENTS

The authors extend our sincere thanks for the financial support provided by the Oregon Department of Transportation (ODOT). In particular the authors appreciated the advice, counsel, and support provided by Ray Bottenberg and Andrew Blower of ODOT, Nuria Ramos and Julio Torres of the Instituto de Ciencias de la Construcción Eduardo Torroja, and Bernie Covino of Corrosion Science & Engineering. We also acknowledge the input and assistance of Rich Wanke and his staff at Great Western Corporation for providing our team members safe access to the several structures what were inspected during the course of this work.

DISCLAIMER

This document is disseminated under the sponsorship of the Oregon Department of Transportation. The State of Oregon assumes no liability of its contents or use thereof.

The contents of this report reflect the views of the authors, who are solely responsible for the facts and the accuracy of the material and information presented herein. The contents do not necessarily reflect the official view of the Oregon Department of Transportation.

The State of Oregon does not endorse products or manufacturers. Trademarks or manufacturers' names appear herein only because they are considered essential to the object of this document.

This report does not constitute a standard, specification, or regulation.

CATHODIC PROTECTION EVALUATION

LIST OF TABLES

LIST OF FIGURES

1.0 INTRODUCTION

1.1 BACKGROUND

U.S. 101, which runs along the shore of the Pacific Ocean, is one of the foremost scenic highways in America. This stretch of coastal highway includes eleven conventionally reinforced concrete bridges designed by Conde B. McCullough. Two of the bridges investigated during this work are listed on the National Register of Historic Places.

Much of this coastline includes areas with beautiful and constant breaking surf. These picturesque waves produce saltwater mist that the wind carries to the bridges and there contaminates the concrete with chloride ions. The chloride ions diffuse through the concrete, and when they reach a threshold concentration at the level of the reinforcing bars, corrosion of the steel commences. The resulting corrosion product occupies greater volume than the original steel producing stress in the concrete surrounding the steel. In time, those stresses build to a sufficient level and crack and spall the concrete cover.

To address the problem of reinforcing steel corrosion, the Oregon Department of Transportation (ODOT) has employed cathodic protection (CP) on a number of their coastal bridges. ODOT's first application of CP was installed in 1985 on the north approach of the Yaquina Bay Bridge and employed an electrically conductive carbon-based paint (*Laylor, 1989*). Today ODOT is a world leader in the field having applied CP to over a million square feet of concrete (107,000 m²) (*Tinnea & Cryer, 2008*), and that effort continues (see Table 1.1).

Table 1.1: Oregon Bridge Cathodic Protection Systems

		AREA		
BRIDGE	**INSTALLED**	**m²**	**ft²**	**ANODE TYPE**
Yaquina Bay: North Approach	1985	645	6,945	Carbon Coating
Cape Creek	1991	9,530	102,580	Thermal Spray (TS) Zinc
Yaquina Bay: Arches	1994	18,170	195,580	TS Zinc
Depoe Bay	1995	5,940	63,940	TS Zinc
Depoe Bay	1995	280	3,015	TS Titanium
Yaquina Bay: South Approach	1997	6,041	65,025	TS Zinc
Cape Perpetua	1997	57	615	TS Zinc
Cape Perpetua	1997	57	615	TS Aluminum Zinc Indium
Cape Perpetua	1997	57	615	Zinc Hydrogel
Big Creek	1998	1,865	20,075	TS Zinc
Cummins Creek	2001	1,865	20,075	TS Zinc
Rocky Creek (Ben Jones)	2001	3,700	39,825	TS Zinc
Rogue River (Patterson)	2003	33,000	355,210	TS Zinc
Tenmile Creek	2007	1,372	14,770	TS Zinc
Lint Creek Slough	2010	74	800	Discrete Zinc
Coos Bay (Conde McCullough)	2011	24,406	262,705	TS Zinc
Pistol River Bridge	2013 estimate	2,811	30,255	TS Zinc

ODOT's first CP system, was installed on the north approach of the Yaquina Bay Bridge. Performance was evaluated using embedded molybdenum-molybdenum oxide reference electrodes using a 100 mV depolarization criteria in accordance with generally accepted criteria at the time. To measure the depolarization, a data logger was connected to a reference electrode, the rectifier was interrupted, and the potential was observed for 1 to 1½ hours (*Laylor, 1989*). The average initial energizing current density was 0.85 mA/ft², which after one month operation was reduced to 0.55 mA/ft², and to 0.28 mA/ft² after one year (*Tinnea & Cryer, 2008*). Unless otherwise noted, current density is expressed in terms of anode surface area, as opposed to the area of the embedded reinforcement. Since that initial project, ODOT has adopted a current density of 0.2 mA/ft² as a general operating level for their impressed current cathodic protection (ICCP) systems (*Bullard, 2009*).

1.2 PROBLEM STATEMENT

Proper operation of a CP system requires the ability to be able to accurately monitor performance. A system providing an inadequate level of protection allows some continued reinforcement corrosion that can lead to cracking and spalling of concrete and steel section loss. A CP system that provides current well in excess of that needed for protection reduces its own service life for no gain in performance. Ponding of water can result in localized excesses of CP current that can produce acidic reactions at the anode-concrete interface, which attack the concrete as shown in Figure 1.1 (*Broomfield & Tinnea, 1992*). Beyond possible damage with no gain in performance, overprotection consumes excessive AC power.

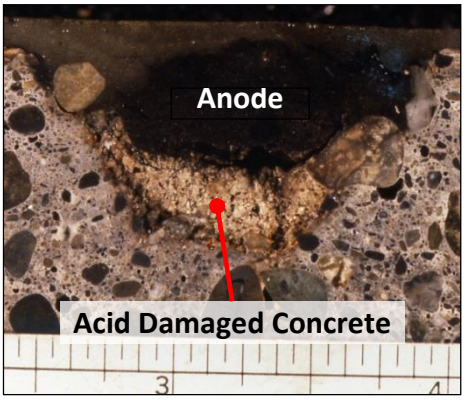

Figure 1.1: Acid Attack at Anode Surface

ODOT bridge CP systems are typically evaluated using several metrics including:

1. Depolarization at locations where permanent reference electrodes are installed.
2. Evaluation of null probes (present on some bridges).
3. Close interval potential surveys.
4. Rectifier output parameters such as volts and amps.

Each of these evaluation and system monitoring techniques has its own characteristics:

1. Depolarization
    a. Can provide accurate evaluation of the level of protection
    b. "Instant off" (per NACE SP0290 from 0.1 to 1 seconds) can be tedious to define exactly.
        i. A "too soon" value can lead to underprotection.
        ii. A "too late" value can lead to overprotection.

c. Essentially, the test should terminate when no further significant depolarization is expected.

d. Per NACE SP0290, how long a time is required to properly conduct a depolarization test largely depends on "…oxygen availability at the reinforcement surface and is not a reflection of the efficiency of the CP system." For this reason SP0290 does not cite a specific interval for conducting depolarization tests.

   i. One to four hours can work well for uncoated concrete, exposed to the air, and with shallow to moderate concrete cover.

   ii. Longer periods of monitoring the depolarization, sometimes greater than 24 hours (*Tinnea, 1998*), are required to evaluate CP for reinforcement embedded in coated, low permeability, or water-saturated concrete.

2. Null Probes

   a. Although installed in some of the earlier ODOT TS zinc ICCP systems, null probes have proven to be difficult to use in the field and are now seldom used (*ACI 222R*).

3. Close Interval Potential Mapping

   a. Close interval potential mapping can be used, but the technique requires access to the concrete surface, and on most cathodically protected ODOT bridges, could only be used to measure potentials of the top mat of deck reinforcement.

4. Use of Fixed Output

   a. Galvanic anode cathodic protection (GACP) systems essentially operate in a fixed voltage output mode.

   b. ICCP rectifiers are available that can be operated in either constant current or constant voltage mode.

   c. Constant Current Operation
      i. Requires relatively complex electronics that can be problematic in field operation.
      ii. If a conservative output value is employed, the CP system may overprotect at times.

   d. Constant Voltage Operation
      i. Does not require special electronics.
      ii. The output varies in response to changes in the concrete resistivity.
      iii. TS zinc anodes are known to develop an increase in resistance as a function of electrochemical aging (*Covino, 2002*).
      iv. Excessive increases in circuit resistance might lead to underprotection.

The Gecor 9 is a test instrument that has potential to address some of the CP system monitoring problems noted in above four points. The Gecor can employ both alternating current (AC) and

direct current (DC) electrochemical techniques to evaluate reinforcement corrosion activity. Given that the Gecor employs somewhat sophisticated methods to measure corrosion activity, there is a question as to its practicality for field use by individuals who do not have a background in electrochemistry.

1.3 OBJECTIVES

There were two main objectives for this work. The first was to evaluate the Gecor 9 and see if it could be employed as a means to improve ODOT's ability to monitor their bridge CP systems. The second was to see if the Gecor 9 could evaluate the condition of embedded reinforcement in two ICCP zones that had prematurely failed.

To achieve these goals, the work included the following tasks:

- A critical evaluation of the Gecor 9 corrosion rate meter as a tool to help ODOT in maintaining and monitoring its cathodically protected bridges.
- An investigation of current control and voltage control as rectifier operational modes for recently installed ICCP zones at the Coos Bay Bridge.
- An investigation of the effectiveness of embedded GACP installed at the Lint Creek Bridge.
- An evaluation of the corrosion activity of reinforcing steel in a failed ICCP zone at the Yaquina Bay Bridge.
- A report that clearly and concisely reports the field data, the findings, and inspector's conclusion and recommendations regarding the four items immediately above.

1.4 REPORT ORGANIZATION

As a starting point, the next section provides a brief discussion of CP methods employed by ODOT to protect their bridges. It also discusses what happens within the reinforced concrete matrix as a result of long-term operation of CP systems. Section 3 provides a discussion of the methods and equipment employed during the multiple field evaluations. Section 4 is a summary of the work findings, while Section 5 provides our conclusions and recommendations for ODOT. Appendices include detailed drawings of the locations where testing was conducted, and extended test data tabulations.

2.0 CATHODIC PROTECTION OF OREGON BRIDGES

2.1 CORROSION OF REINFORCEMENT

2.1.1 Introduction

In conventionally reinforced concrete, the steel reinforcing bars are known as rebars. Typically, concrete protects the embedded rebar from corrosion. This protection is not provided by concrete acting as thick paint and isolating the steel from the weather. Rather it is from the concrete being very alkaline. The Portland cement that binds the aggregate and rebar produces a high pH environment, with values typically >12.5. Most rebar is made from carbon steel, and in such an alkaline environment, the corrosion behavior of carbon steel is similar to that of stainless steel. This behavior is known as passivation, and involves the formation of a thin, but protective, oxide layer forming on the steel surface. This passive film will remain stable as long as the pH is > 12 and no aggressive ions, like chlorides, are present. Rebar in a passive state has a corrosion rate that is so low it has no significant impact on the rebar structural ability or the reinforced concrete service life.

2.1.2 Chloride Penetration of Concrete

Certain aggressive ions, like chlorides, can disrupt the passive film that protects the rebar and initiate corrosion at pH values above 12. Chloride ion contamination of concrete is typically from the presence of seawater or deicing salts.

Figures 2.1a through 2.1c show the process of chloride ion penetration into the concrete, to corrosion initiation, and then the loss of concrete bond and cracking that spalls the concrete covering the corroded rebar. In the outer ½ to ¾ inches of concrete, capillary suction usually dominates chloride movement, while at greater depths diffusion dominates.

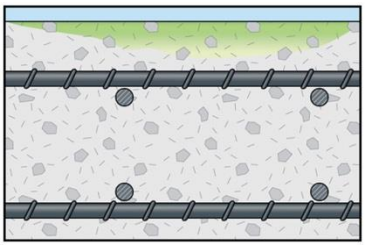

Figure 2.1a: Chloride Penetration

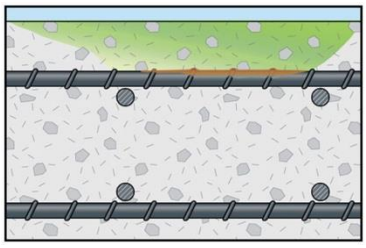

Figure 2.1b: Corrosion Initiation

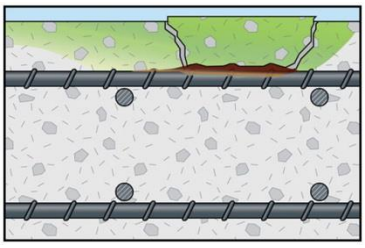

Figure 2.1c: Spalled Concrete

Figure 2.1a shows chloride ions migrating into the concrete from the surface. The relative intensity of the green color reflects the concentration of the chloride ions, with the darker green at the surface reflecting a higher concentration of chloride ions than the pale yellowish green at greater depth. Figure 2.1b shows the situation when the chloride ion concentration at the top rebar mat reaches the corrosion threshold concentration. The exact concentration varies, impacted by oxygen availability, pH, and concrete electrical resistivity. A light layer of rust can be seen on the top of the top bar. As corrosion progresses, Figure 2.1c shows that in time the rust layer thickens and the resulting stress in the concrete produces cracks, spalls, and potholes.

2.1.3 Damage from Reinforcement Corrosion

When chloride ions present at the steel surface reach the corrosion threshold, the rust that forms on the rebar occupies up to eight times the volume of the metallic iron that corroded and formed that rust. This increase in volume produces tensile stresses that after sufficient corrosion will crack the concrete. Depending on the depth and spacing of the rebar, these cracks may form perpendicular to the concrete surface and immediately above the corroding rebar or the crack may form parallel to the surface of the concrete and at the level of the rebar.

If the concrete cover over the rebars is relatively shallow, or the rebars are widely spaced, cracks form that are aligned with the rebars and are perpendicular with the concrete surface as shown in Figure 2.2.

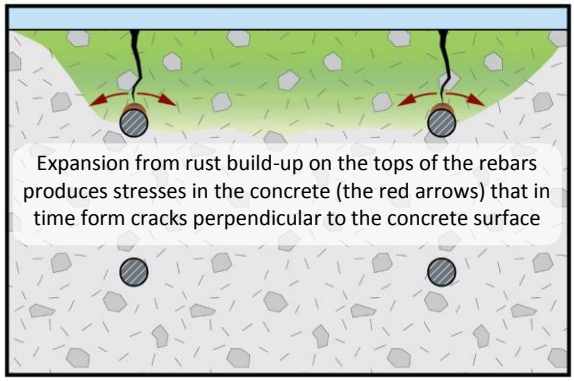

Figure 2.2: Rust Layer Cracks the Concrete

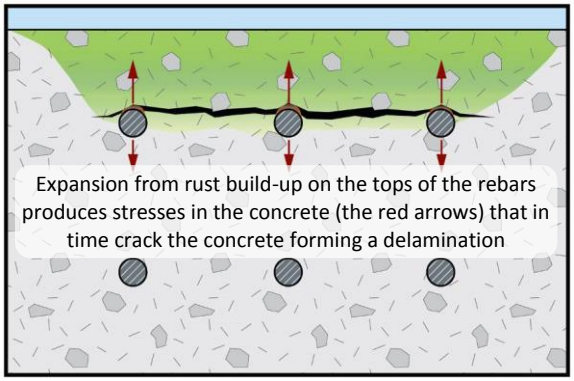

Figure 2.3: Rust Delaminates the Concrete

If the concrete cover over the rebars is relatively deep, or the rebars are closely spaced, cracks form parallel with the concrete surface. Initially these cracks are not visible from the surface but they can be detected by traditional sounding using a hammer or steel chain and are known as delaminations (see Figure 2.3). When struck, delaminated areas sound hollow if the delamination is not filled with water.

2.1.4 Identifying Reinforcement Corrosion

2.1.4.1 Electrolytes

NACE International and ASTM in 'Standard Terminology Relating to Corrosion' (*NACE/ASTM G 193, 2009*) define an electrolyte as:

> *A chemical substance containing ions that migrate in an electric field.*

Outside of chemistry labs, common electrolytes include water (both fresh and saltwater), fruit juice, and blood. Electrolytes are also present in materials we consider as solids including soil and even concrete. When a metal surface is exposed to an electrolyte it will exhibit a voltage known as a corrosion potential across the metal-electrolyte interface. The voltage produced is reflective of the corrosion activity occurring on the metal surface. To measure the corrosion potential of a metal requires the use of a reference electrode that has a stable and reproducible potential.

2.1.4.2 Corrosion Potentials

Figure 2.4 illustrates the use of a reference electrode to measure the corrosion potential of a rebar embedded in concrete. The reference electrode is placed on the concrete surface and connected to the negative terminal of a high impedance voltmeter (>10 MΩ). The rebar is connected to the positive terminal of the voltmeter, and the voltage between the rebar and reference electrode is then measured.

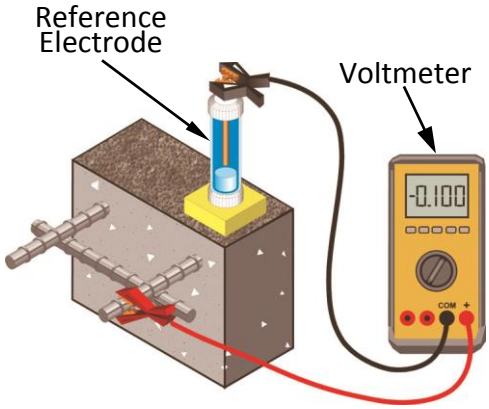

Figure 2.4: Field Measurement of Corrosion Potential

It is important to recognize that measurement of rebar corrosion potentials in the field inherently includes greater errors than electrochemical measurements made in a laboratory. In the lab, devices called Luggin probes allow potentials to be measured within 0.04-inches (1 mm) or closer. See Figure 2.5 for a typical laboratory setup with a counter electrode (CE) that is used to polarize the working electrode (WE). The polarization is followed by the reference electrode (RE) fitted with a Luggin probe. The tip of the Luggin is capillary size and allows readings to be made quite close to the WE surface. In a CP system the rebar would be the WE, the anode would be the CE, and polarization of the rebar/WE is followed by using either portable or permanent reference electrodes/REs. With the presence of the overlying concrete, this simply is not possible in the field.

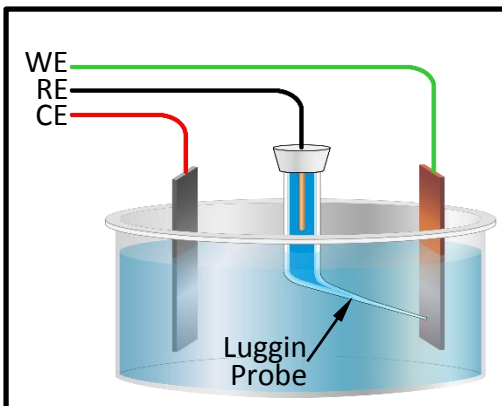

Figure 2.5: Laboratory Measurement of Corrosion Potential

Figure 2.4 shows a field measurement with the RE placed on a conductive contact material such as a sponge placed on the concrete surface. The potential that the RE "sees" in a single reading is an average of corrosion potentials along the length of the adjacent rebar as shown in Figure 2.6. How much of adjacent rebar is included in any one reading depends on several factors including:

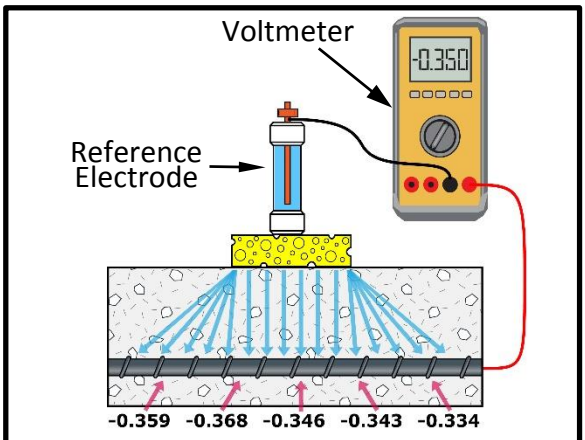

Figure 2.6: Corrosion Potential is an Average

- Depth of concrete cover
- Concrete resistivity and variations of same
- Size of the contact material

Note that in Figure 2.6, the measured reading of -0.350 mV is an average of the five readings shown below the bar. This is a simplified case, and actual practice. The total resistive path from the rebar surface to the reference electrode plays a significant role. Locations further from the center of where the reference is placed have a greater resistive path to reach the reference electrode than do locations directly under the electrode. This

attenuates how much of the rebar corrosion potential at a distance is included in the observed readings. So in actual field readings, locations closer to the reference electrode receive greater weighting in the measured value (*Tinnea & Feuer, 1985*).

Another factor that will influence the observed reading derives from a potential that results from wetting of the concrete by the conductive contact material. This derives from the fact that as the water moves through the concrete, not all of the ions travel at the same rate of speed. When anions and cations are moving at different speeds as the sponge wets the concrete, an electrical charge can develop in the concrete. This charge is between the reference electrode and the rebar, and is included in the voltmeter reading which is often referred to as a junction potential. Figure 2.7 shows how a junction potential develops.

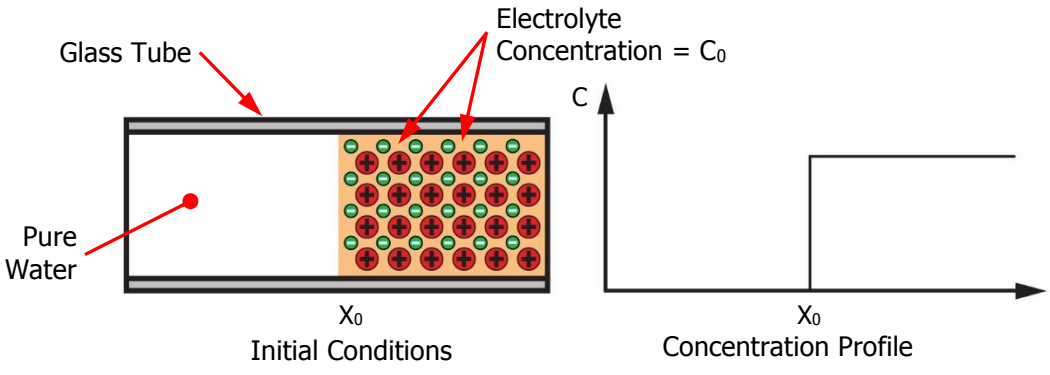

Figure 2.7a: Junction Potential Initial Conditions

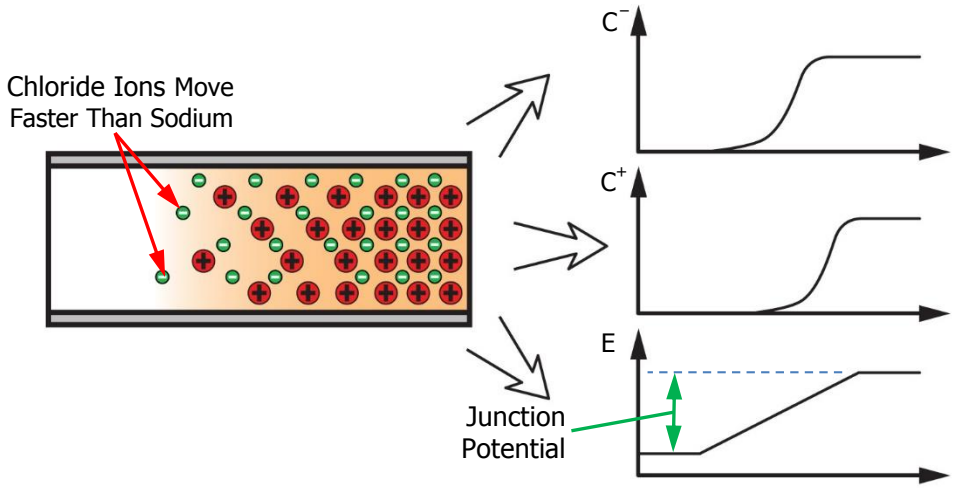

Figure 2.7b: Junction Potential While Wetting

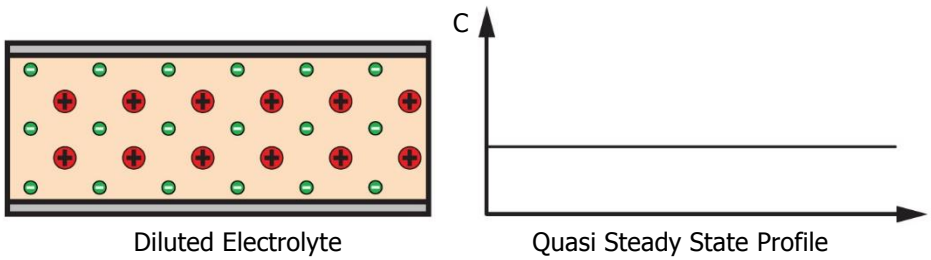

Figure 2.7c: Junction Potential Final Steady State

Figure 2.8 shows how the potential changes over time from the moment the sponge is placed on the concrete surface. Note the difference in behavior between the saturated sponge and damp sponge. In addition to the relative wetness of the sponge, or other conductive contact material, the concrete surrounding the rebar also plays a behavior role that is largely governed by moisture content (*Tinnea, 1991*).

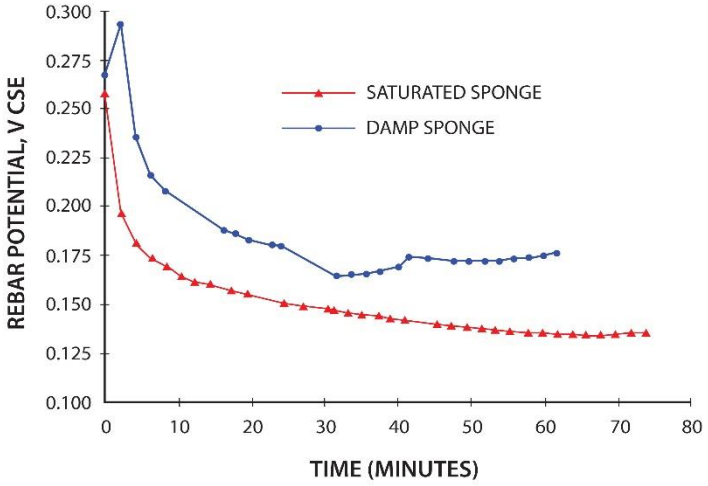

Figure 2.8: Variation in Reading Due To Junction Potential

To address junction potential errors, ASTM Standard C876 and NACE Standard Practice SP0308, both require the investigator to check for stability of the readings prior to initiating a potential survey and pre-wetting if necessary. ASTM Standard C876 provides guidance on surveying the corrosion potentials of rebar embedded in concrete, including that the reading remain "…stable (± 0.02V) when observed for at least 5 minutes." Although the absolute value of the corrosion potential of rebar can provide a general sense of corrosion activity, the observed potential can be affected by temperature, pH, and oxygen availability. For example, in water-saturated concrete the corrosion potential may be shifted in the negative direction by several hundred millivolts from what would be the case for rebar in the same concrete were it atmospherically exposed. This depression in corrosion potential is the result of reduced oxygen availability.

It is clear that it is not possible to obtain laboratory precision with field measurements of rebar corrosion potentials. ASTM C876 states to report rebar potential readings to the nearest 0.01V, and in Section 12, Precision and Bias, states:

- The difference between two readings taken at the same location with the same reference electrode should not exceed 10 mV
- The difference between two readings taken at the same location with two different reference electrodes should not exceed 20 mV.

2.1.4.3 Mapping Potentials

Fortunately in most modern reinforced concrete construction, redundant wire ties and crossing of bars provides very good electrical continuity between adjacent rebars allowing large areas to be tested with a single rebar connection.

If the rebar corrosion potentials are collected at known positions on the concrete surface, then the location, X and Y, can be plotted against the potential, Z, to generate a map of the rebar corrosion activity. This approach is similar to the creation of topographic maps where elevations are plotted against northing and easting. In corrosion potential maps, the contours reflect lines of equipotential instead of elevation contours.

To identify localized corrosion activity requires mapping rebar corrosion potentials on a relatively close interval of 6 to 12 inches. To obtain this data by chalking a grid on the surface, recording the voltage measurements by hand, and then entering the data into a mapping software program would be extremely tedious and expensive. Figure 2.9 shows a wheeled reference electrode and data logger used for data collection. If parallel lines are marked on the concrete surface, then the wheel electrode can be run along the surface of the concrete and the data automatically recorded at pre-set intervals that are measured using the shaft encoder and the diameter of the reference electrode wheel. The data so collected can be used to produce potential maps useful in identifying areas of corrosion activity and for locating reference electrodes useful in monitoring cathodic protection systems.

Figure 2.9: Potential Mapping

Although it is not possible to obtain rebar corrosion potentials as precisely in the field as it is in the lab, if collected properly the information gained is both informative and important from a property management standpoint. Figure 2.10 is a potential map obtained at the old Conde McCullough designed Alsea Bay Bridge (*Tinnea & Feuer, 1985*). Note that the map of corrosion potentials is essentially a stress map for the beam. Also note in the area circled that the potentials change by over 300 mV in less than one foot. This is why in ASTM C876 states "two readings taken at the same location with the same reference electrode **should** not exceed 10 mV" (emphasis added). In areas with dramatic change in corrosion potential, obtaining exactly the same potential at the same location may be difficult, but there is a clear reason for this behavior and it is not a reflection that either the method or the inspector's technique are flawed. The authors have used rebar corrosion potential mapping to identify rebar with localized full-section corrosion loss in areas where traditional sounding indicate there is no corrosion damage (*Tinnea, 2002*).

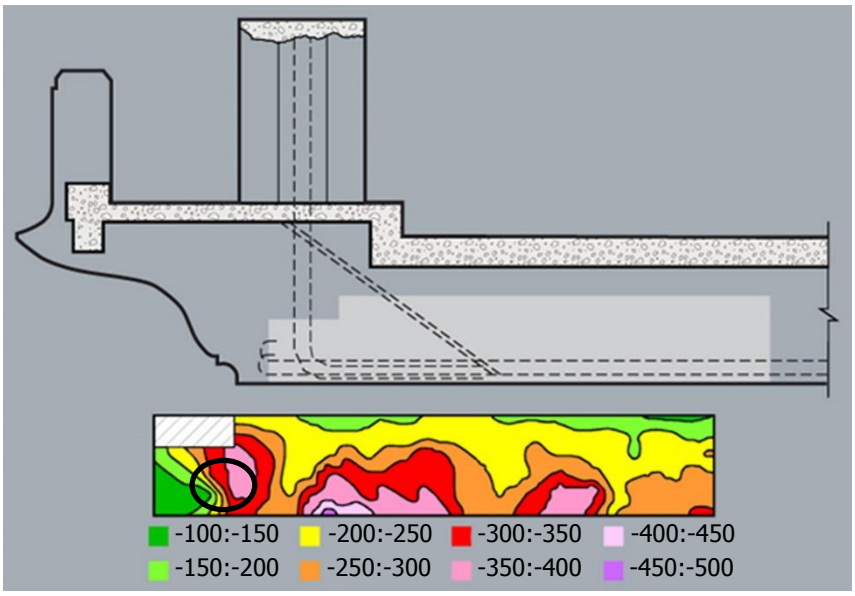

Figure 2.10: Map of Corrosion Potentials (mV)

2.1.5 Corrosion Rate Testing

Mapping of reinforcement corrosion potentials can identify areas of likely corrosion with relatively minimal destructive requirements needed to secure an electrical connection to the steel reinforcement grid. While potential maps can quickly and inexpensively identify areas where

steel corrosion is likely present, such maps do not provide quantifiable information on general corrosion rates that are present (*Escalante, 1990*). Reasonably accurate information on current corrosion rates could be used to provide a basis for estimates of future corrosion activity and time to cracking or spalling. Clearly, techniques that can provide a means to quantifiably assess reinforcement corrosion without requiring the removal of concrete would be valuable to highway agencies and other owners of potentially corroding reinforced concrete structures.

Historically, field corrosion rate testing of steel embedded in concrete was time consuming and provided data that was not particularly reliable. Several factors contributed to this and include:

- The high electrical resistance of the electrolyte – the concrete
- The presence of macro cells – anodic and cathodic areas present in close proximity to each other that produced localized corrosion currents flowing in the concrete
- Uncertainty as to the surface area of the embedded steel that contributed to the readings
- If CP was present, extended depolarization is necessary to perform DC techniques (*Broomfield & Tinnea, 1992*)

2.1.5.1 DC Techniques

For reinforced concrete where there are not strong macrocell corrosion currents, such as in the immediate area of localized corrosion and abrupt changes in the rebar corrosion potential, traditional DC polarization techniques can be employed to measure the rebar polarization resistance (R_p).

Using R_p measurements to determine the corrosion rate of metals was first reported by Stern and Geary (*Stern & Geary, 1957*). They defined R_p as the change in a metal's potential divided by the change in current ($\Delta E/\Delta i$). The basic relationship is the Stern-Geary equation:

$$i_{corr} = \frac{(\beta_a \times \beta_c)}{2.3 \times (\beta_a + \beta_c)} \times \frac{\Delta i}{\Delta E} = \mathrm{B}\frac{\Delta i}{\Delta E} = \frac{\mathrm{B}}{R_p} \qquad \textbf{Eqn 1}$$

The corrosion current is $\boldsymbol{i_{corr}}$ $\boldsymbol{\beta_a}$ and $\boldsymbol{\beta_c}$ are, respectively, the anodic and cathodic Tafel slopes, $\boldsymbol{\Delta i}$ and $\boldsymbol{\Delta E}$ are the measured changes in current and steel potential. The equation can be simplified, as shown above, where **B** is a function of the Tafel slopes and $\boldsymbol{R_p}$ is the quotient of $\boldsymbol{\Delta E \div \Delta i}$.

Basic Configuration

As R_p is the change in the embedded steel's potential divided by a change in current crossing the steel-concrete interface, it stands that we can deduct i_{corr} by effecting small changes in either the potential of the steel or the current crossing the steel-concrete interface and then observing changes that occur in the other. In a fashion similar to CP rectifiers, such testing can be conducted galvanostatically (current control) and potentiostatically (voltage/potential control).

Figure 2.11 shows a general layout for conducting measurements made by altering the reinforcement potential, (ΔE) **,** and then observing how much current was required to accomplish that change (Δi), or the reverse. As mentioned above, in electrochemical parlance, the embedded steel reinforcement is known as the working electrode (WE). A counter electrode (CE) is used to

apply an electrical current to the WE from a power supply that can accurately measure small current flow. A reference electrode (RE) and the WE are connected to a high impedance voltmeter to measure changes in potential.

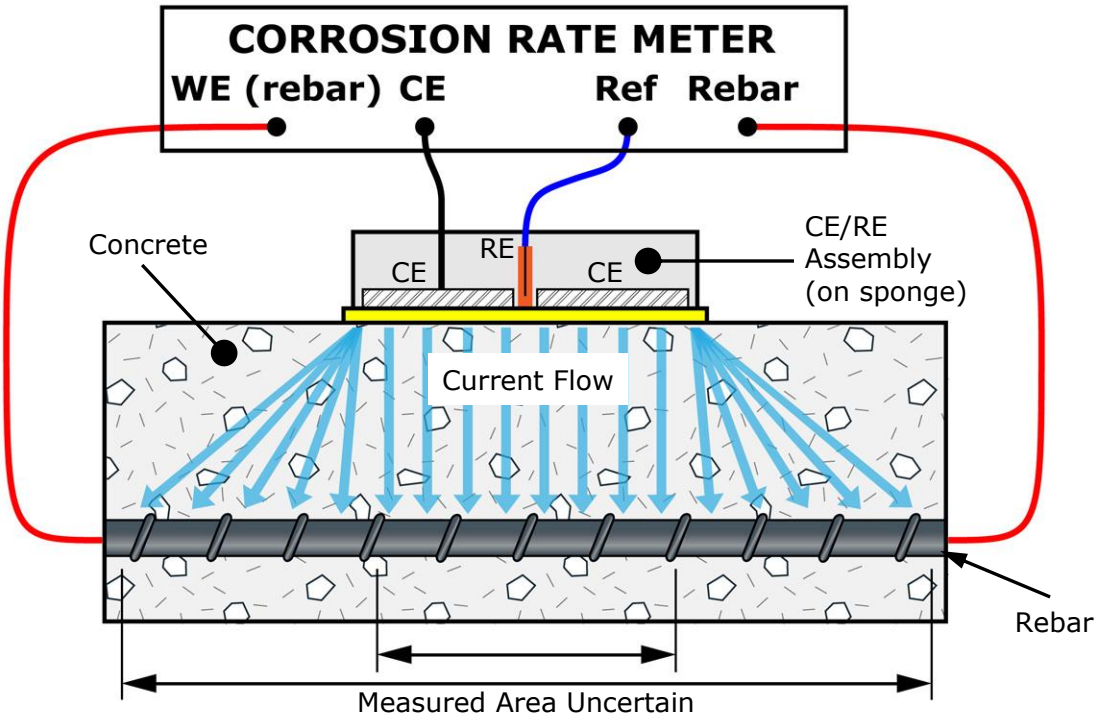

Figure 2.11: Schematic Polarization Test Configuration

Note in Figure 2.11 that the current flowing from the CE to the WE, the rebar, is shown spreading beyond the "footprint" of the CE. How far this current will spread directly depends on the resistivity of the concrete and the depth of concrete cover. With conditions as shown above, the concrete resistivity and depth of cover can produce a wide variation in the surface area of the steel being polarized. Although we accurately measure the potential change versus the current output, not knowing the surface area responsible for those changes introduces a non-trivial error in making calculations of the actual corrosion rate (mA/sq ft) of embedded reinforcement.

Several approaches have been employed to make estimations of the surface area of the steel polarized during the test. One approach is to make empirical estimations based upon previous findings, and CE and steel geometry (*Clear, 1987*). However, any estimates of the steel corrosion rate will deviate from the true value by the magnitude of any error in the estimate of the steel surface area that was polarized.

Use of a Guard Electrode

A second approach is to use a guard electrode (GE) which is a ring-shaped electrode concentric to the CE. The concept is that by polarizing the GE in lockstep with the CE the GE will polarize the rebar adjacent to the area being investigated. The GE polarizing the adjacent rebar will confine the CE signal, reducing the CE signal attenuation and thereby improve estimation of the rebar surface area polarized. The GE concept was first suggested for application to concrete by Escalante et al (*Escalante, 1980*). Work on development and evaluation of the GE continued in the 1980s (*John, 1987*). The GE is typically powered by a buffer amplifier that follows the voltage driving the CE

and is thus often referred to as a 'voltage follower.' Figure 2.12 shows a simple schematic of a polarization test configuration that includes a GE. Note that with this arrangement the current flowing from the GE helps to confine current flowing from the CE. The confinement produced by employing a GE improves the operator's ability to estimate the area being polarized.

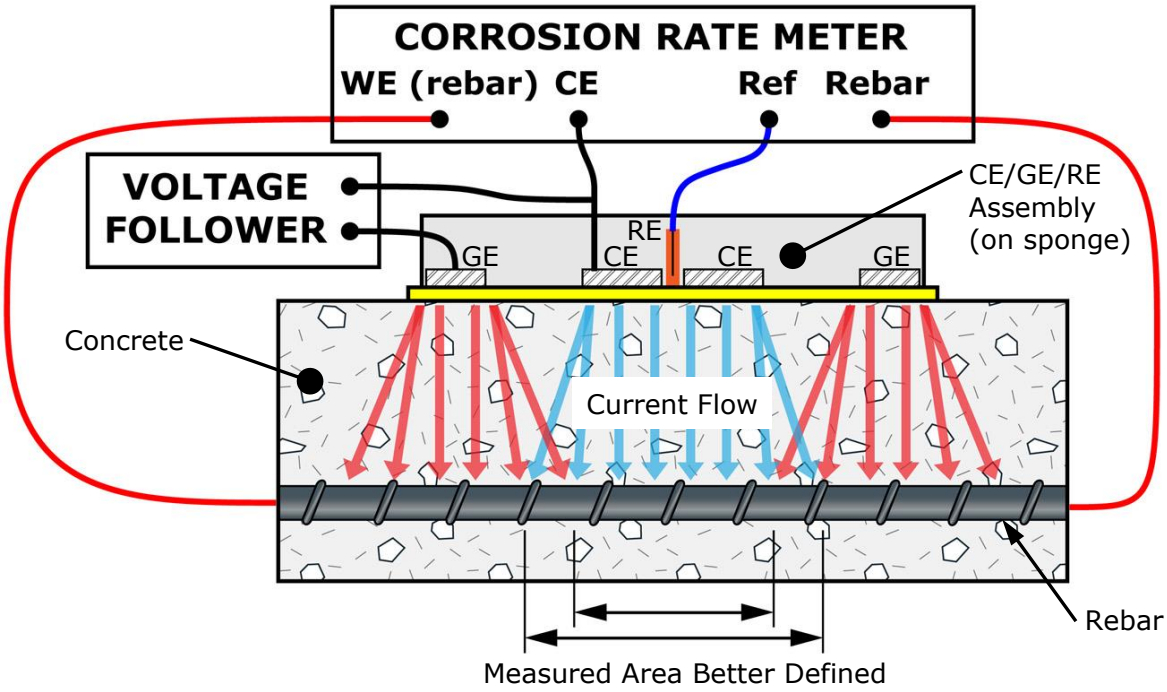

Figure 2.12: Schematic Polarization Test Configuration with Guard Electrode

Linear Polarization Resistance

The simplest DC corrosion rate test method is linear polarization resistance (LPR). In this procedure, predetermined steps of current (Δi) or potentials (ΔE) can be applied by the CE. The resulting changes in current or potential, whichever is the non-controlled variable, are measured and those measurements allow estimates to be made of the steel reinforcement corrosion rate. Typically, the measurements are taken stepwise, after a fixed time interval following each polarization step. The step approach is used for LPR measurements of rebar corrosion rate, because reactant transport in the concrete is slow, and the steps allow the current and potential to reach a quasi-steady state condition. By employing equipment with a GE, the investigator can make a better estimate of the surface area of the steel being tested than is possible with a non-GE arrangement.

Linear Tafel behavior is generally valid in the range of from ±5 to ±20mv from the free, or "open circuit" potential of the steel reinforcement. R_p is the slope, $\Delta E/\Delta i$, of the linear plot of the rebar potential versus current applied near the free corrosion potential.

To convert an R_p measurement to a corrosion rate requires also knowing the surface area that was polarized. Equation 2 shows the formula to convert such a measurement into a corrosion rate.

$$x = \frac{k \times \mathrm{B}}{R_p \times A} \qquad \textbf{Eqn 2}$$

Where x = corrosion rate (μm/yr), k is a constant (11.53×10^{-3}), **A** is the surface area of steel being polarized, and **B** and $\boldsymbol{R_p}$ are as before.

Work by Feliu and others showed that incorporating the GE worked well if the steel was corroding and the R_p value was low, but the arrangement tended to understate R_p values for reinforcement in a passive condition (*Feliu, 1990a*).

To improve the performance Feliu and his co-workers revised the GE arrangement by adding two additional reference electrodes between the CE and the GE (*Feliu, 1990b*). This configuration, which is similar to that of the Gecor 9, is shown in Figure 2.13. In addition to adding REs to assist in GE control, the instrument measures the resistance between the RE and the steel reinforcement.

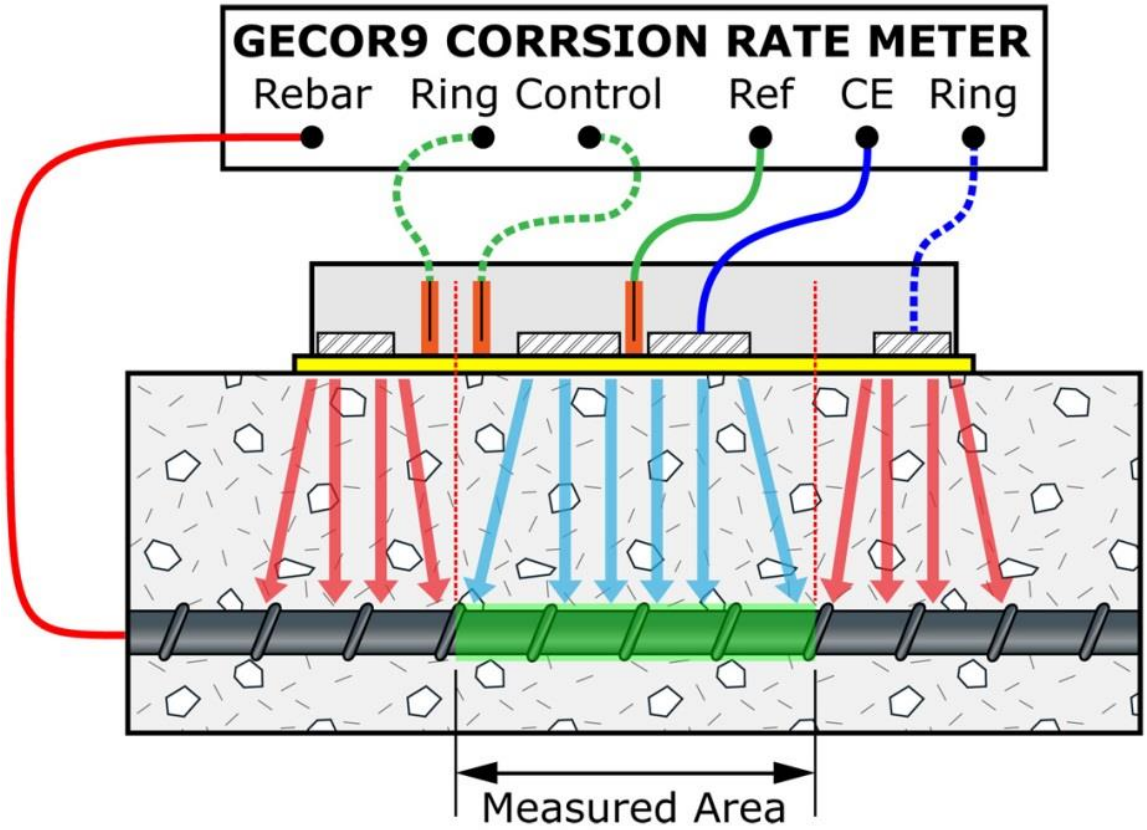

Figure 2.13: Gecor 9 Test Configuration with Guard Electrode

In Figure 2.13, the two additional reference electrodes are shown at the left and are connected to the two ring control terminals. The difference in potential between these two references is used to improve the precision of the GE output to better confine the CE output.

By more clearly defining the area polarized and measuring the resistance between the RE and the embedded steel, R_p is now defined by:

$$R_p = \left(\frac{\Delta E}{\Delta i} - R_e\right) \qquad \textbf{Eqn 3}$$

$\boldsymbol{R_p}$, $\boldsymbol{\Delta i}$ and $\boldsymbol{\Delta E}$ are as before and $\boldsymbol{R_e}$ is the ohmic resistance between RE and the steel. This approach improves estimation of the measured area and removes the effect on accuracy the value of R_p.

Short Duration Pulses

The corrosion current density, i_{corr}, can also be ascertained by applying short duration pulses (SDP) of potential or current. The short duration of these pulses provides a time-of-measurement advantage over typical LPR testing. In addition, by disrupting the embedded steel for a much shorter period there is less likelihood of changing conditions at the steel-concrete interface with SDP as can occur with LPR (*Bastidas, 2007*).

Figure 2.14 shows a simplified Randles equivalent circuit (EC) that is similar to what is being tested when one attempts to measure the corrosion rate of steel embedded in concrete, where $\boldsymbol{R_\varepsilon}$ is the bulk resistance of the concrete, $\boldsymbol{C_{DL}}$ is the double layer capacitance at the steel-concrete, and $\boldsymbol{R_p}$ is as before. Note that C_{DL} and R_p are in parallel with each other, and that the pair is in series with the CE, R_ε, and the WE.

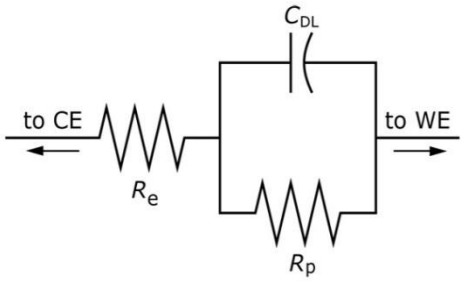

Figure 2.14: Randles EC for Steel-Concrete

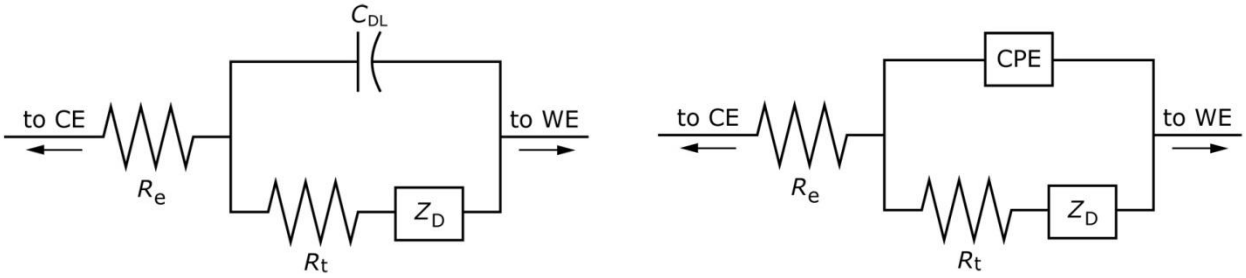

Figure 2.15: More Exact Equivalent Circuits for Steel-Concrete

Figure 2.15 shows more complex circuits have been proposed that provide more exact electrical representation of the steel-concrete interface, where R_e is the electrolyte resistance; R_t is the charge transfer resistance; C_{DL} is the double-layer capacitance; Z_D is the Warburg diffusion; CPE is the constant phase element (*Feliu, 1996*; *Feliu, 1998*). In both of these representations a Warburg diffusion process, Z_D, is included to represent oxygen diffusion to the cathode. In the figure at the right, the capacitive double layer, CDL, is replaced with what is called a constant phase element (CPE). Since the double layer often does not behave like an ideal capacitor, Sagüés et al. proposed that the C_{DL} be replaced with a CPE, a generalized impedance element that can range in behavior from a perfect capacitor to a perfect inductor (*Sagüés et al, 1996*).

Gecor 9 Corrosion Rate Testing

The Gecor 9 derives from that work that sought to limit attenuation of the current between the CE and the embedded reinforcement (WE) by using a GE. The Gecor 9 employs a galvanostatic approach measuring Rp and the rebar corrosion rate. The Gecor 9 assumes the constant B has a value of 26 mV.

2.1.5.2 AC Techniques

For rebar that may be suffering severe localized corrosion and rebar that is under cathodic protection, the Gecor 9 can measure the corrosion rate using a variation of AC techniques that are typically only used in the laboratory.

When significant DC currents are present, they interfere with LPR testing and preclude its use. These DC currents can come from macrocells or from the application of CP. AC test measurements can be conducted in the presence of DC currents from other sources, but historically a large spectrum of AC frequencies were scanned and this took far too much time to conduct in the field and where conditions in the concrete are dynamic.

To work around this, the Gecor uses five fixed frequencies for its AC-based passivity verification technique (PVT) (*Andrade, 2002; Martinez, 2007*). While this procedure is not as rigorous as AC-based electrochemical impedance spectroscopy (EIS) performed in the lab, it has the advantage of being field doable and is not at the mercy of dynamic weather conditions during tests that could run an hour or more. The AC test provides semi-quantifiable corrosion condition test results for CP and can also be used to flag localized corrosion.

The PVT provides a categorical evaluation of the performance of the CP system, not quantitative results. Depending on the response, the Gecor's PVT method classifies the reading as well protected, moderately protected, or non-protected. Including set-up and measurement time, each of these readings takes from 12 to 15 minutes. Compared to from 4 to over 24 hours for depolarization testing, this technique is quite rapid.

2.2 CATHODIC PROTECTION OF STEEL IN CONCRETE

Cathodic protection is one method to stop future concrete cracking, delamination, and spalling by controlling the cause: corrosion. The general corrosion process is similar to that of a battery. Cathodic protection, also known as CP, is a technique that is in some ways similar to a battery charger, reverses the normal flow of electric current and in the process makes the formerly corroding anodic rebars into non-corroding cathodes.

The electrical current that provides CP comes in two sources. The first is galvanic and employs sacrificial anodes. These galvanic anodes are familiar to boat owners in the form of zinc anodes that are attached to the propeller or rudder of a boat. It is also commonly used in the form of galvanizing. To galvanize a nail or guardrail, the steel element is dipped into molten zinc. Historically galvanic anodes have been used to protect steel piling in marine environments and buried pipelines and tanks.

Galvanic anodes are fabricated from metals that are more electrochemically active than the metal that is being protected. When the galvanic anode is attached to the metal to be protected, a corrosion battery is created where the anode corrodes and by that process cathodically protects the other metal from corrosion. To protect steel, galvanic anodes are typically fabricated from special alloys of aluminum, magnesium, or zinc. A disadvantage with GACP systems is they have a fixed output voltage that may be insufficient to power CP systems applied to reinforced concrete in all conditions.

CP can also be provided by an electronic DC power supply. Configurations of this type are referred to as impressed current systems. Most ICCP systems utilize a rectifier. An advantage to impressed current CP systems is that when necessary, the output voltage can be increased to overcome the electrical resistance of the concrete.

There are many factors in deciding which type of CP system should be used to protect a reinforced concrete structure. These include the geometry of the structure or areas requiring protection, the expected resistance of the concrete, and cost. Aesthetics are also a consideration.

2.2.1 Overview

As mentioned above, the corrosion process is similar to that which produces electricity in a battery. CP is a method of controlling corrosion that operates in a fashion similar to that of a battery charger. Like a battery charger, a CP system forces electricity to flow in the opposite direction than would be the case of normal battery operation. The general goal of an effective CP system is to polarize the potential of the cathodic areas present in the structure to be protected to the open-circuit potential of the most anodic area. For example, say the corrosion potentials for a concrete slab had been obtained on a 6-inch by 6-inch grid, and the most anodic potential (most negative reading) was -0.350 V, measured to a copper-copper sulfate electrode (CSE). To fully protect that slab, the goal would be to polarize all of the locations in the slab to -0.350 V_{CSE}. Often it is not possible to exhaustively survey a structure, so other techniques are employed in industry-accepted standards for CP criteria.

CP systems for steel in concrete can come in two forms: impressed current and galvanic (see Figure 2.16a and b). With ICCP systems the power to drive the "battery charger" comes from a rectifier. A rectifier is a device that converts AC electricity from a wall outlet into DC. With GACP, an anode material that is more electronegative than the rebar, for example zinc, is used as the anode material. The anode corrodes instead of the rebar and no external power source is required.

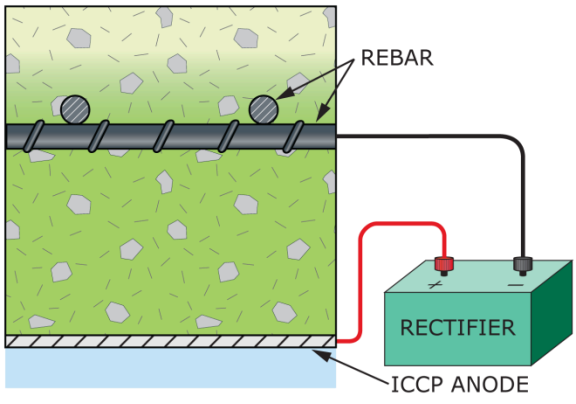

FIGURE 2.16a: ICCP System

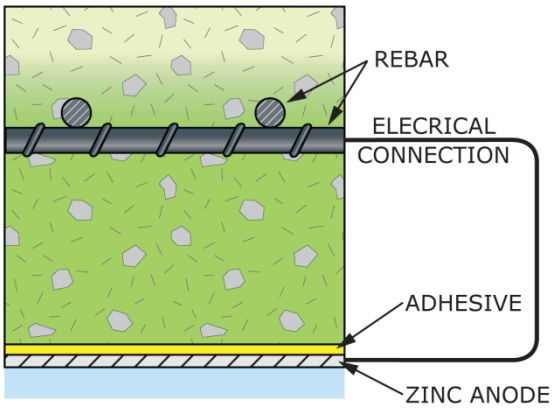

Figure 2.16b: GACP System

Figure 2.16a shows schematic drawing of ICCP system and Figure 2.16b shows a GACP system. In this case both the ICCP and GACP anode are shown fixed at the surface of the concrete structure. ICCP anodes are available that can be installed in grooves or slots cut into the surface of the concrete. Both types of CP systems are available with anodes that can be embedded into the concrete. For example, GACP anodes, often referred to as "hockey pucks" because of their shape, can be placed at the edge of a repair excavation to avoid macrocell corrosion currents resulting from reinforcement exposed to chloride-free repair material and chloride-bearing concrete around the edge of the patch.

Anodes that are applied over the existing concrete surface are called distributed anodes. These anodes can be left on the surface, as is the case with ODOT's TS zinc systems or various saw-slot anode configurations. Distributed anodes may be covered with a cementitious overlay or shotcrete as is done with titanium mesh anodes. Generally with distributed anodes it is assumed that the current density within the CP system zone is relatively evenly distributed. Sometimes that may not be the case. For example, if an area sees frequent ponding of chloride-bearing water the local current density may be many times the "nominal" current density. Significantly uneven current distribution that results from such a case can lead to significant damage to the concrete as was shown in Figure 1.1.

Embedded anodes are typically point anodes. These can be installed within the confines of repair excavations on by drilling holes in the concrete and installing the anodes there. Generally point anodes are installed on elements with relatively small geometry, say a bridge beam or areas of building framing, while distributed anodes are employed on larger elements like bridge decks and piers.

The choice of using ICCP or GACP depends on a number of factors. These include, but are not limited to, initial cost, life-cycle cost, on-going maintenance demands, environment, power availability, and properties of the concrete. As with many engineering decisions, there is not one size that fits all.

- If repairs are being made to a structure with a relatively short estimated future service life, then embedded GACP anodes installed in the patches might provide a proper solution to extend the service life of the repairs by avoiding what is known as halo corrosion around the patch, but CP is not provided to the whole structure.

- If a conventionally reinforced bridge with integral beams is only showing corrosion on the beams and a longer relative service life is desired, the embedded GACP anodes can be installed at regular intervals in drilled holes. The grid spacing depends on the level of chloride contamination and the steel density.

- If larger areas of a bridge are suffering corrosion-related distress, then a distributed anode system is likely the appropriate choice. Selection of the best type of distributed anode to employ depends on location, geometry, frequency of immersion or wetting.

Beyond basic geometry and service life considerations, several other decision factors pertinent to the selection of ICCP or GACP systems are tabulated below:

the selection of ICCP or GACP systems are tabulated below:

Table 2.1: CP System Decision Factors

ITEM	ICCP	GACP
Initial Cost	Relatively high	Relatively low
Life Cycle Cost (>30 years operation)	Relatively low	Relatively high
On Going Maintenance Demands	Relatively high	Relatively low
High Resistivity Concrete	Can increase voltage	May be a problem
Acid Attack of Concrete at Anode	Occurs with ponding	Not a problem

Table 2.1 applies to typical installations, and specific installation conditions may produce variations to what is listed.

2.2.2 What Happens with Time

When CP is applied to the hull of a ship operating in the Pacific Ocean, the passage of CP current from the anode to the ship's hull does not significantly affect the chemistry of the ocean. Conversely, when CP is applied to concrete structures, the flow of current produces profound changes to the chemistry at the rebar surface that will impact future corrosion behavior.

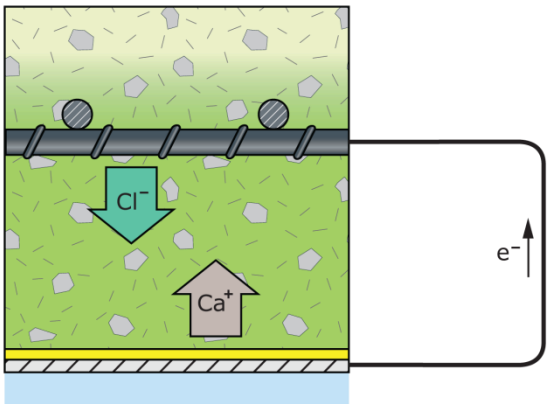

Figure 2.17a: Initial CP Current Flow

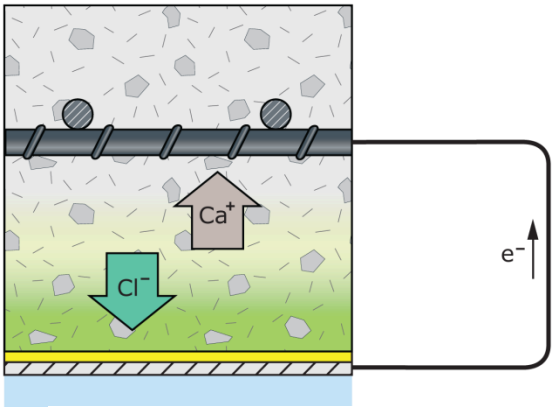

Figure 2.17b: Later CP Current Flow

When a CP system is applied to protect rebar in concrete, an electric current flows in the system. In metal components, like the rebar and wires, the flow of that current is through the moving of electrons shown as e^-. In the concrete, however, the flow of electric current is through the migration of ions. Anions, like chloride ions (Cl^-), move toward the anode, and cations, like calcium (Ca^+) flow to the cathode, which is the rebar. This initial case is shown in Figure 2.17a where the green coloring of the concrete indicates chloride contamination. With time, the application of CP will move chloride ions away from the surface of the rebar, as shown in Figure 2.17b. Further, the pH at the steel-concrete interface is increased. The absence of corrosion-accelerating chloride ions at the surface of the rebar means that if the CP current is interrupted it is reasonable to expect that passive behavior would return to the previously corroding rebar.

This return of passivity does indeed occur. This phenomenon was initially reported in a report prepared as part of the US National Academy of Sciences' Strategic Highway Research Program (SHRP) (*Broomfield & Tinnea, 1992*). One means to observe this migration is to look at changes in the concrete chloride concentration as a function of depth from the surface, or source of the chloride ions. This can be especially informative if there are adjacent exposure areas both with and without CP. Figure 2.18 shows the chloride ion concentration as function of depth for two adjacent areas on the same bridge (*Broomfield & Tinnea, 1992*). The two profiles are for samples obtained from the conductive carbon-doped coating ICCP system located on the North Approach of the Yaquina Bay Bridge. One curve is for a core sample obtained in an area with CP. The second profile is for a core obtained in an area without CP. Note that the profile for the with CP concrete shows significantly lower chloride levels than the adjacent area without CP. The migration of the chloride ions as a result of the passage of CP current returns the environment of concrete surrounding the reinforcement to one that will support passivity and no significant corrosion of the steel. It should be noted that with carbon-doped coating anodes, chloride ions can be converted to chlorine gas at the anode-concrete interface (*Cramer, 2002*), and hence there is no large build-up of chloride at the anode such as occurs with TS zinc anodes (*Covino, 2002*).

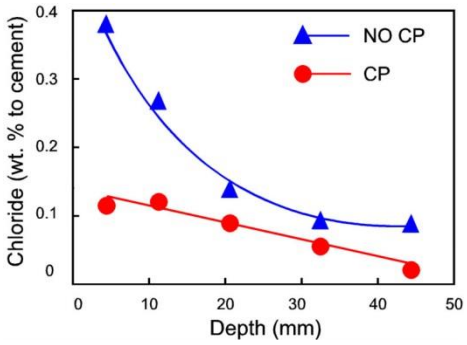

Figure 2.18: Chloride Profile vs. Depth

In areas generally protected from repeated washing by direct exposure to rain, you can actually see the chloride building-up on the structure surface. Figure 2.19a shows a deck with a carbon-base anode saw slot ICCP system. The saw slot anodes run left and right. Perpendicular to the saw slots are white deposits that exactly align with the upper rebar in the top mat in the deck. In Figure 2.19b, white deposits can be seen around primary anodes on the Cape Creek Bridge. In both cases lab testing confirmed the white deposits principal anion was chloride.


FIGURE 2.19a: ICCP System


Figure 2.19b: ICCP System

In the general case for concrete, the chloride threshold for steel corrosion depends on pH of the concrete pore water, oxygen availability, chloride concentration, and temperature. In total, this is difficult to graph, so Figure 2.20 shows a plot of the reinforcement corrosion rate as a function of sodium chloride concentration in neutral solution (*Fink, 1960*). Note in Figure 2.20 that at NaCl concentrations just under 10 g/l, that oxygen solubility starts to drop. Also note that as the oxygen solubility starts to drop, so too does the relative corrosion rate of iron, the principal ingredient of steel.

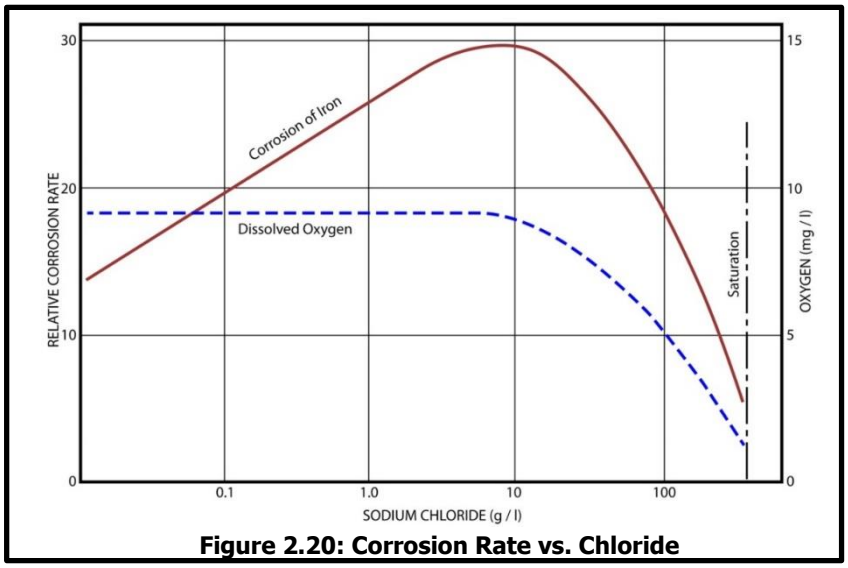

Figure 2.20: Corrosion Rate vs. Chloride

Work at the National Institute for Standards and Testing (NIST) has shown that the corrosion of steel in concrete is dependent upon pH, the availability of oxygen and the presence of chloride ions, or other aggressive ions such as carbonate (*Escalante, 1984*). NIST prepared a chart showing the relationship between oxygen concentration, chloride ion concentration, and pH. Figure 2.21 shows the relationship between pH, oxygen concentration, and chloride content and corrosion of steel reinforcement. Note that an increase in oxygen or chloride concentrations and reductions in pH will increase steel corrosion activity.

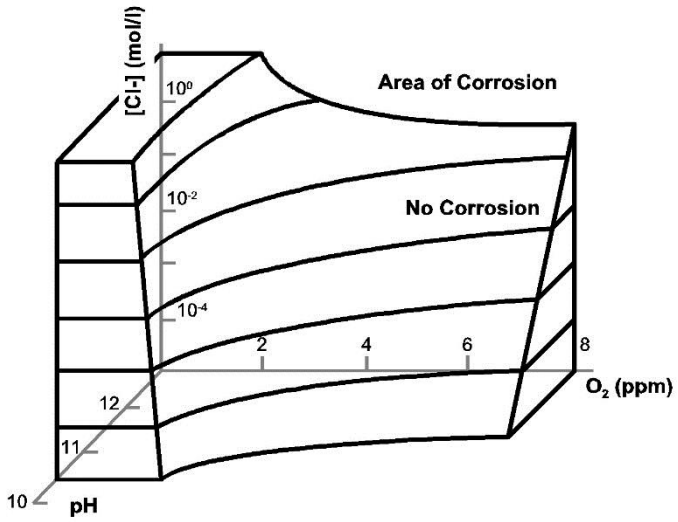

Figure 2.21: Corrosion Rate vs. pH, O_2, and Cl

2.2.3 Polarization Reduces Corrosion

The above-cited SHRP report discussed several cases where CP systems that had been in operation were turned-off for periods of up to 90 days. These close-interval potential surveys indicated all of the rebar had been returned to passive, non-corroding conditions. Further, repeated potential surveys showed no return to active corrosion in any of the areas that had previously been receiving CP. This is not behavior that would typically be seen with CP of steel in seawater or steel buried in the soil. Clearly, the behavior of steel under CP in concrete differs from CP of steel in other common environments.

When CP is properly applied to a metal, the application of the CP current shifts the potential of the protected metal in a negative direction. That potential shift is accompanied by a reduction in the rate the metal is corroding through a decrease in the corrosion current. If the change in potential is plotted against the log of the corrosion current, the result is generally linear behavior unless there are impediments in the transport of reactions (e.g. availability of oxygen at the metal surface). In soil and seawater applications of CP, the slope of this line is typically less than 100 mV/decade of current. The mV/decade is referred to as the anodic Tafel slope, βa. Therefore, in traditional applications of CP, a polarization of 100 mV will reduce the corrosion rate by over an order of magnitude. Figure 2.22 (*Cramer, 2003*) shows how 100 mV polarization from C_{corr} to CP by connecting a rebar, Fe, to a zinc anode, Zn, reduces the corrosion rate by over an order of magnitude. For most applications that level of reduction is sufficient to provide the desired degree of corrosion control.

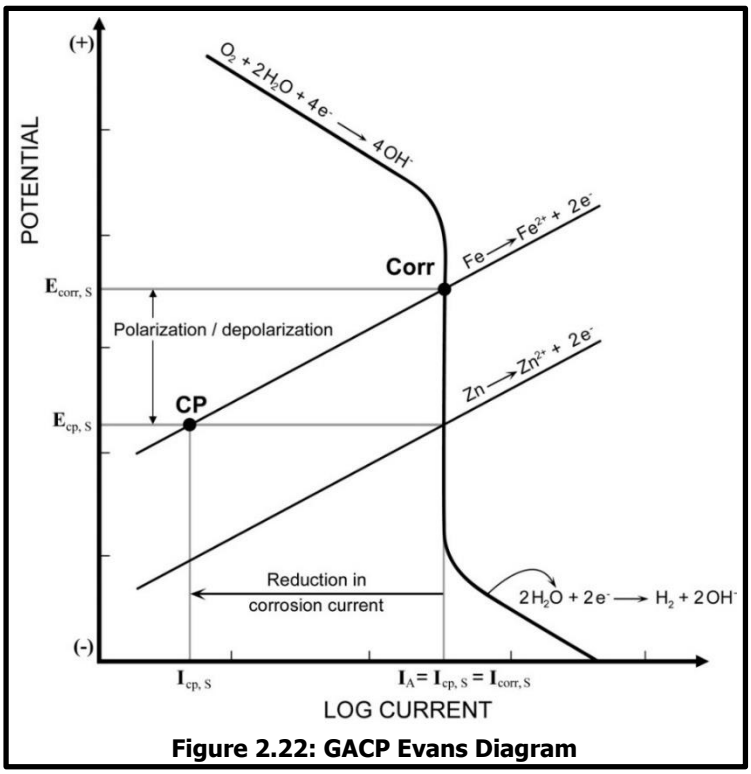

Figure 2.22: GACP Evans Diagram

2.2.4 Polarization in Concrete

Figure 2.23 (*Tinnea, 2006*) is a map of corrosion behavior with the corrosion potential being the Y axis and the pH shown on the X axis. This type of corrosion behavior presentation is known as a Pourbaix Diagram. Starting a point P, the rebar exhibits passive behavior in concrete with a high pH and no chlorides. Moving to point A, the rebar is corroding. This is either due to a loss of pH, typically through carbonation, or corrosion activity brought on by chloride ion contamination destabilizing the passive oxide film and the steel corrosion process locally reducing the pH of the concrete.

The initial application of cathodic protection at point CP_i will provide protection through polarization as shown in Figure 2.23, the pH of the concrete. With time, the application of the protective current will cause chloride migration away from the rebar (see Figures 2.17b and 2.18) and/or realkalize the concrete by increasing the

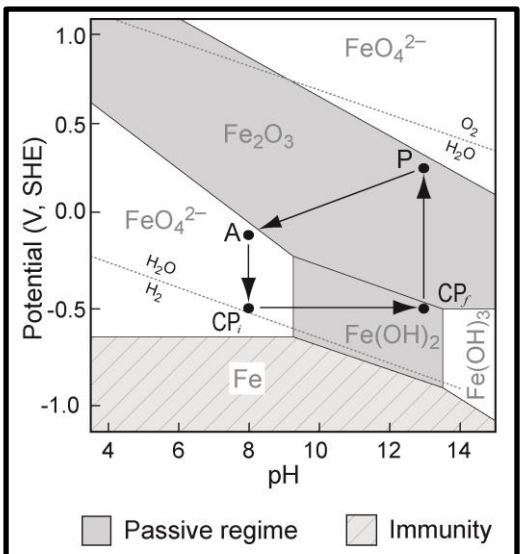

Figure 2.23: Corrosion Path of Steel

local pH at the rebar surface shown by point CP_f. At this point, if one were to disconnect the CP system, the rebar would return to the passive condition shown by point P.

Absent chloride ions or loss of pH to carbonation, the steel will exhibit passive behavior shown by point P in Figure 2.23. Once corrosion initiates, the corrosion process follows similar behavior to steel in seawater, but the process is still affected by concrete's tortuous pore structure and the alkaline environment. For these reasons there are two distinct regimes of Tafel behavior. Figure 2.24 shows that for passive non-corroding reinforcement a βa > 700 mV/decade is expected, while for corroding reinforcement βa < 120 mV/decade is observed (*Glass, 2003*). These large differences in anodic Tafel behavior have significant impact on the proper application of protection criteria when evaluating CP systems on reinforced concrete structures. Returning to Figure 2.23, note the generalized passive and active regimes delineated with respect to potential and pH, and consider how the very anodic Tafel slopes in Figure 2.24 define the same behaviors in terms of potential and corrosion rate.

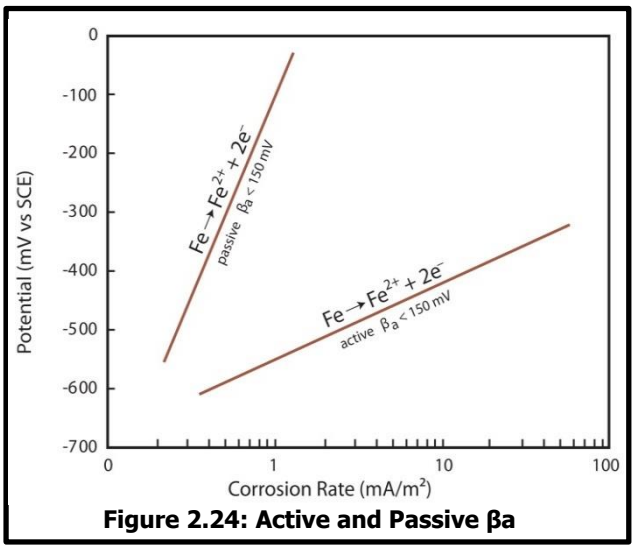

Figure 2.24: Active and Passive βa

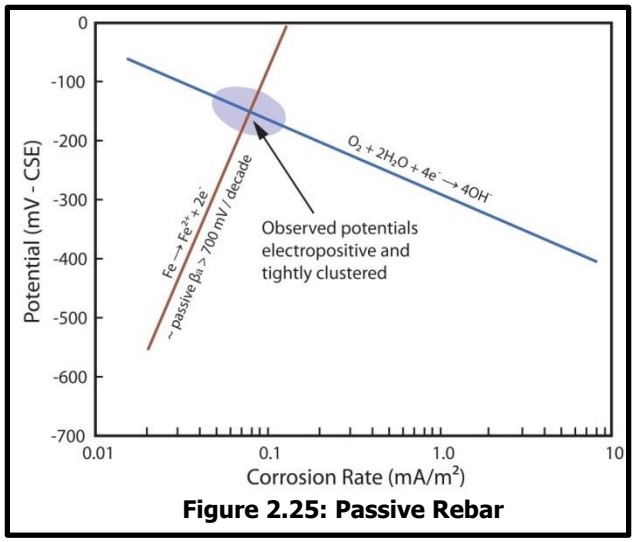

Figure 2.25: Passive Rebar

Figure 2.25 (after *Glass, 2001*) shows an Evans diagram for embedded rebar in a passive state. Note that the Tafel slope βa for iron corrosion is 700 mV/decade. Also note that the observed potentials are tightly clustered about where the anodic $Fe \rightarrow Fe^{++}$ line intersects the cathodic $O_2 + 2H_2O + 4e^- \rightarrow 4OH^-$ line.

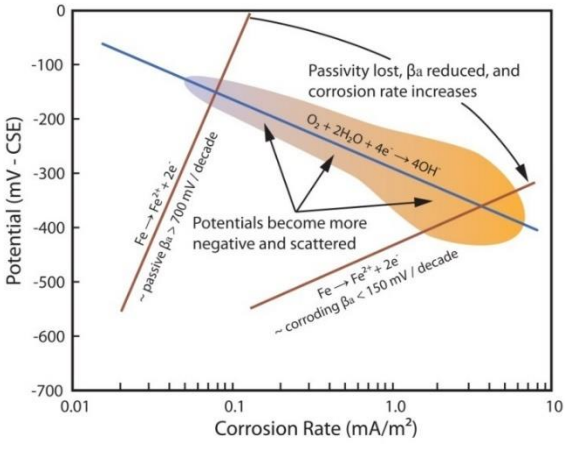

Figure 2.26a: Transition to Corroding Rebar

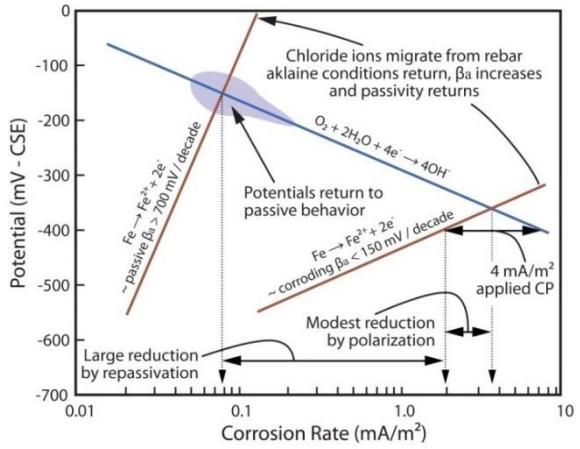

Figure 2.26b: Return to Passive Rebar

Figure 2.26a illustrates the transition from the reinforcement in passive state, shown in Figure 2.25 to an actively corroding state with a βa for iron corrosion of about 120 mV/decade (after *Glass, 2001*). Note that the distribution of rebar potentials has become more broad and negative. Figure 2.26b shows how after the application of CP for some time, if the system polarization is allowed to fully decay, the rebar potentials return to passive-like values and distribution.

After a reinforced concrete CP system has been energized for several years, it can take months to fully depolarize. Figure 2.27a shows a plot of the average reinforcement potential obtained over a three month period after the system was turned off (*Broomfield & Tinnea, 1992*). Each average reading is comprised of over 200 readings taken on a 5-foot grid over an entire zone. The first data point is the average of "immediate off" readings obtained 0.5 seconds after interrupting the rectifier with a programmable interrupter. After the "immediate off" readings were obtained, the rectifier was actually turned off and additional data sets collected at 3 hours and 2, 7, 36, 43, 72, and 90 days. Note that after about a month after the CP system was turned-off the rebar potentials reflect values ASTM C876 identifies with passive rebar and even after 90 days off the potentials are showing no sign of returning to active corrosion.

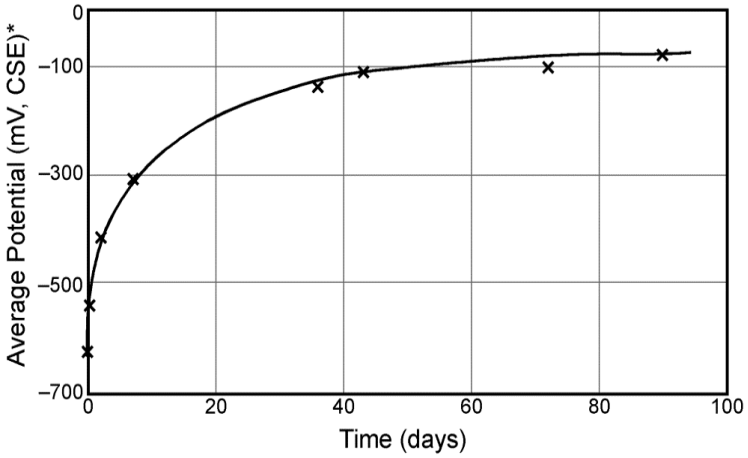

Figure 2.27a: Extended CP System Polarization Decay

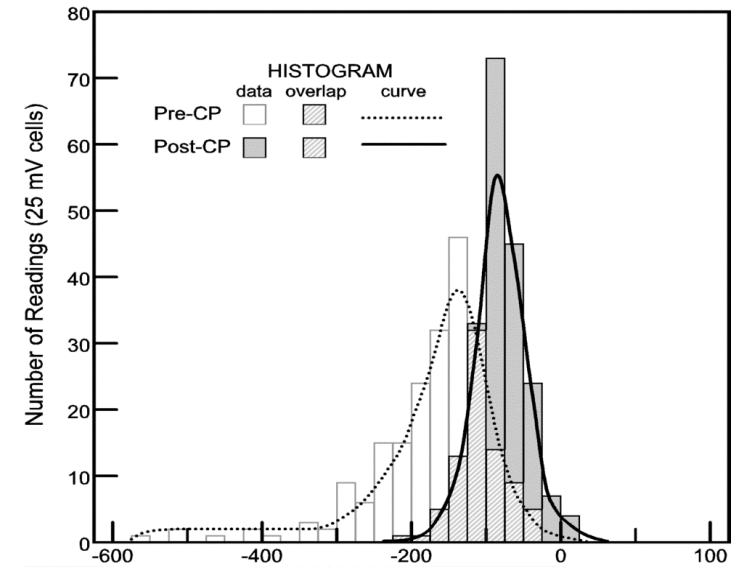

Figure 2.27b: Pre CP and Post CP Decayed Potential Histograms

Figure 2.27b shows histograms of rebar potentials obtained before the CP system was energized. Also shown is a histogram of the post-CP 90-day depolarized data. Note that the pre-CP corrosion potential histogram is much broader, and includes substantially more negative potentials than does the 90 day depolarized data. This behavior follows what was shown in Figures 2.26a and 2.26b, above.

2.3 ANODE SYSTEMS

Two types of CP systems were investigated as part of this work. The first is the TS zinc ICCP. The second was a GACP system that employs embeddable galvanic anodes.

2.3.1 Impressed Current Cathodic Protection

Two ICCP systems investigated employed TS zinc distributed anode systems. This is a mature technique for ODOT given their first system of this type was installed in 1991 and the Department has approximately one million square feet in operation.

Twenty-one zones of the Coos Bay Bridge were evaluated using the Gecor 9. As this work was conducted during the installation of that system, this location was also used to evaluate the Gecor itself.

Two zones at the Yaquina Bay Bridge were evaluated using the Gecor 9. These were zones where the zinc coating had failed as a result of a rectifier malfunction that caused voltage and current output that was 2 to 7 times higher than the intended set point (*Holcomb, 2002*).

2.3.2 Galvanic Anode Cathodic Protection

The Gecor 9 was also used to evaluate GACP systems installed on beams of the Lint Creek Bridge. The anodes were fabricated from high purity zinc slugs that were cast in a special mortar by the manufacturer. These anodes help to avoid macrocells at the boundaries between patch material and the surrounding concrete in addition to providing general CP in the areas where installed.

2.4 CATHODIC PROTECTION CRITERIA

With their ICCP systems, ODOT installs both embedded reference electrodes and test wells where portable reference electrodes may be used to conduct depolarization testing.

2.4.1 Polarization / Depolarization Criteria

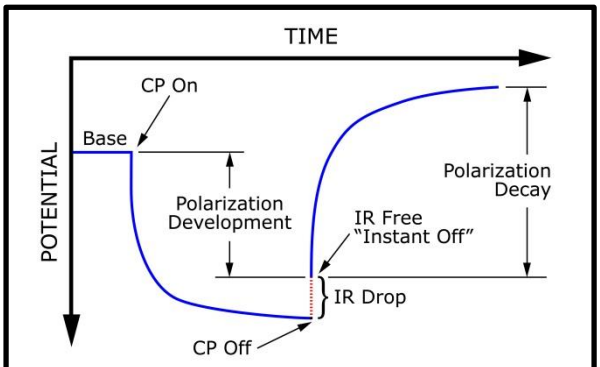

Figure 2.28: Polarization-Depolarization

NACE SP0290 calls for a minimum of 100 mV polarization from native potentials, or 100 mV depolarization from an "Instant Off" reading. The duration of the test can have a clear impact on the values recorded. Per SP0290 the "Instant Off" reading is typically read between 0.1 and 1.0 seconds after the rectifier is interrupted. Readings at times less than 0.1 seconds often include reactive components that have nothing to do with CP. If one waits more than one second, the observed change will be understated. Figure 2.28 provides a stylized diagram. Starting on the left with the base potential before CP is applied the polarization is shown, whereby the steel potential is polarized in a negative, cathodic direction. About midway, the rectifier is turned off and the potential shifts in a positive direction. The area between 'CP Off' and 'Instant Off' include IR error and reactive transients resulting from interrupting the CP current. At a point between 0.1 and 1 second is the start of the depolarization.

All normally encountered electrolytes are resistive. That being the case, Ohm's Law, E = IR, tells us that when CP current (I) passes through the electrolyte (R) a voltage is produced (E). When the CP system is turned off, there can reactive transients that occur from the collapsing magnetic field that surrounds the wires and rebars carrying the CP current. There can also be capacitive transients. Errors from CP current-generated IR and interruption transient currents must be addressed when measuring the corrosion potentials of embedded rebar and when applying DC corrosion rate test methods such as LPR techniques.

Accurate measurements of rebar corrosion potentials should only reflect the potential across the rebar-concrete interface and not include these transient voltages. For reinforced concrete structures the transient are no longer a factor after from 0.1 to 1.0 seconds. If necessary, a precision field portable oscilloscope can used to determine the duration of these transients.

Obtaining accurate measurements of rebar after the application of CP is important. As shown above in Figures 2.26a and 2.26b, after extended operation of a CP system the rebar in a previously corrosion-distressed reinforced concrete structure often exhibits passive behavior as would have been the case prior to chloride ions reaching the steel surface in sufficient concentration to initiate corrosion. This observed behavior supports the concept of operating CP systems on an intermittent basis.

2.4.2 Re-Establish Passive Potentials and Passive Behavior

As was shown in Figures 2.17b and 2.18, the operation of a CP system will cause chloride ions to migrate from the surface of the steel concurrent with alkali migration towards the bars. In time, this process returns the environment surrounding the reinforcement back to conditions that existed prior to chloride contamination. As a result of this migration, it is not surprising that given time to depolarize, the steel would return to potentials reflective of passive conditions. For this reason, NACE SP0290 states "if the corrosion potential or decayed off-potential is less negative than -200 mVcse, then the steel is passivated and no minimum polarization is required."

3.0 FIELD TESTING PROCEDURES

3.1 CORROSION MEASUREMENTS

3.1.1 Potential Measurements

Potential measurements were conducted according to ASTM C876-09. The measurements we obtained using:

- A portable silver-silver chloride (saturated KCl) reference electrode in conjunction with a high internal impedance electronic voltmeter.
- A Proceq SA Canin corrosion analyzing instrument equipped with a copper-copper sulfate (saturated) reference electrode.
- The Gecor 9 corrosion rate meter equipped with a copper-copper sulfate (saturated) reference electrode.

The reference electrodes and voltmeters were checked daily for proper performance. The reference electrodes were checked against a calibrated double junction silver-silver chloride (saturated KCl in inner junction) laboratory reference electrode. The meter voltage readings were checked against those obtained with a calibrated portable voltmeter. The accuracy of the Canin shaft encoder-driven sampling was checked against distances measured with a tape measure. In this report silver-silver chloride readings are converted to copper-copper sulfate equivalents.

3.1.2 Rebar Locating and Depth Measurements

Rebar locating and depth measurements were obtained with an electronic cover meter. Unfortunately, field work showed that cover meters are not able to locate and measure cover depth where TS zinc is present.

3.1.3 Concrete Resistivity Measurements

Concrete resistivity measurements were principally obtained using the Gecor 9. Readings were checked using an AC (97 Hz square wave) resistivity meter and a 4-pin probe.

3.1.4 Corrosion Rate Measurements

Corrosion rate measurements were obtained using the Gecor 9.

3.1.5 Passivity Verification Measurements

PVT measurements were obtained using the Gecor 9.

3.2 THE GECOR 9

The Gecor 9 is a portable device used to evaluate the corrosion condition of reinforced concrete structures. It is able to provide four different measurement techniques that include:

1. Mapping (rebar potential and concrete resistivity)
2. Corrosion rate measurements of atmospherically exposed structures
3. Corrosion rate measurements of very wet or submerged concrete
4. Evaluation of structures with cathodic protection

3.2.1 Components

The Gecor 9 has five major components including the corrosion meter and three types of sensors:

Gecor 9: The meter used to perform and record the testing

Sensor A: Used to obtain polarization resistance (R_p) and for testing protection levels of CP systems.

Sensor B: Used to map reinforcement corrosion potentials and concrete resistivity.

Sensor C: Use for measurements in submerged or very wet concrete (not used).

Dummy: A dummy cell to check on Gecor operation

Figure 3.1: Gecor 9 Components

Figure 3.1 shows the equipment used in this investigation. Sensor A was used to conduct measurements of rebar corrosion rate at Coos Bay and Yaquina Bay Bridges. It was also used to evaluate the effectiveness of the ICCP system at Coos Bay and the GACP system at Lint Creek. Sensor B was used to measure rebar corrosion potentials, concrete resistivity, and make estimates of corrosion risk. Sensor B was used to obtain pre-CP baseline data at Coos Bay and as part of the corrosion condition evaluation at Yaquina Bay.

On each day the Gecor 9 was used, the dummy cell was use to verify proper operation of the Gecor 9. In addition a portable laboratory reference electrode and voltmeter were used to verify the reference electrodes in Gecor sensors were providing valid data. Proper calibration and system performance verification are critical to obtaining meaningful data from a sophisticated test instrument such as the Gecor.

Table 3.1 provides review of the several sensors used by the Gecor.

Table 3.1: Gecor Sensor Operation

	Sensor A	Sensor A	Sensor B	Sensor C
Method	i_{corr}: modulated confinement	CP Evaluation: passivity verification	Mapping: E_{corr}, ρ, and corrosion risk	i_{corr}: potential attenuation
Electrochemical technique	Galvanostatic pulse	Limited EIS (5 frequencies)	Galvanostatic pulse	Potentiostatic pulse
Pulse duration	30 to 100 seconds	n / a	1 to 2 seconds	20 to 80 seconds
Pulse magnitude	5 to 999 µA	n / a	5 to 999 µA	100 mV
Pulse selection	automatic	automatic	automatic	automatic
CE diameter	Central: 70 mm Ring: 180 mm	Central: 70 mm Ring: 180 mm	20 mm	20 mm
No. of electrodes	3 ref, 1 counter, 1 guard electrode	3 ref, 1 counter, 1 guard electrode	1 ref, 1 counter	4 ref, 1 counter
Parameters	i_{corr}, E_{corr}, ρ, R_p	Passivity verification	E_{corr}, R_p, corrosion risk	i_{corr}, E_{corr}, ρ, R_p

3.2.1.1 The Meter

The meter, shown in Figure 3.2, is a portable unit. It is 12"w × 8.25"d × 6"h, and weighs about 12.2 pounds without the 2 pound cover. It has a 5-$^3/_{16}$" × 3-$^3/_8$" 320×240 point liquid crystal display. There is a 14 pin metric circular connector that is used to connect the meter to either one of the three sensors or the dummy cell. There is an RS232 connector that allows direct connection to a computer. There is also a PCMCIA slot for a card to store data. If desired, that card may be removed and then accessed using a card reader connected to a computer. The lead wires needed to connect the sensors and dummy cell are protected by a rugged weatherized sheathing and terminate with weather-tight cylindrical pin-type connectors.

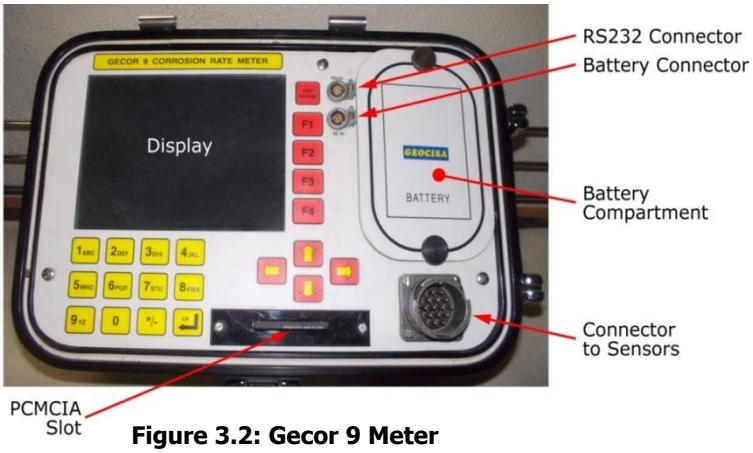

Figure 3.2: Gecor 9 Meter

The Gecor 9 is powered by a nominal 12V, 5Ah nickel-metal hydride (NiMH) battery. There is also a connector to charge the battery while it is in the meter chassis or, as we had to do during

this work, to provide external power. The battery can also be removed and charged outside the meter using an adapter.

The team had recurring problems with the nominal 12V NiMH battery. Sometimes we had to pull the battery and then reseat it to get the meter's internal software to boot. That problem was resolved after returning the instrument to Spain for repairs.

During follow-up testing we had problems with the NiMH battery being able to power the Gecor 9 for a day's testing. This was a nontrivial nuisance that required us to power the Gecor using the battery charger while using the instrument in the field.

Subsequent to the project we discovered that NiMH batteries can develop what is known as a 'memory effect' where if the battery's charge is only partially used several times, then in the future only that small portion of the charge will be available. To overcome this memory effect we used a power resistor to fully draw-down the battery over a period of 12 or more hours, recharged the battery, and then repeated that full draw-down and recharge process several times. After the several iterations of draw-down and recharge we were able to correct the 'memory' effect and again be able to access the full capacity of the battery.

The NiMH battery weighs 4.4 pounds, so it contributes about one third the total weight of the meter. Although not part of this work, the research team considered replacing the NiMH battery with a lithium ion battery because that battery is light weight, has a higher energy density than NiMH, and has no 'memory' effect issues (*Linden & Reddy, 2011*). It should be noted that there are some restrictions on carrying lithium ion batteries on commercial airlines, but the battery size required to power the Gecor would meet those current restrictions.

3.2.1.2 Sensor A

Sensor A is used for two test procedures: 1) measuring the corrosion rate of metals embedded in concrete; 2) evaluating the level of protection afforded by CP systems without interrupting the rectifier output to the CP system being evaluated.

The main body of Sensor A is 7 inches in diameter and 1⅛ inches high and is made from methyl methacrylate. It has a handle on the back that extends about 2 inches out from the main body (see Figure 3.1).

Figure 3.3 shows the face of Sensor A that abuts the concrete surface during testing. At the center of Sensor A is a 2¾ inch diameter stainless steel CE. Along the circumference, note the stainless steel GE.

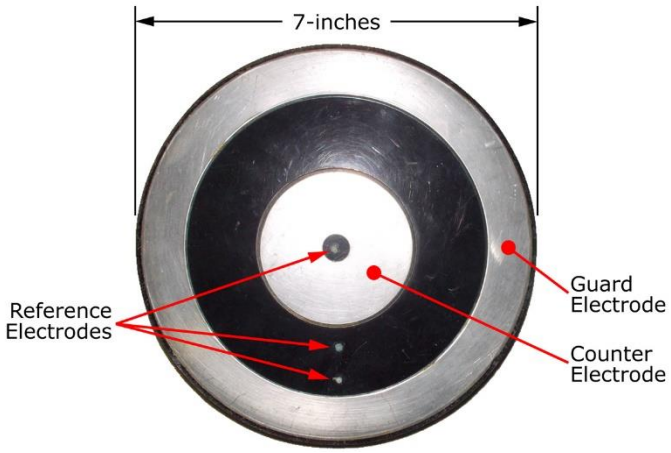

Figure 3.3: Face Sensor A

The unit has three reference electrodes. The unit used in this work was fitted with CSE references. Silver-silver chloride electrodes are also available. One electrode is located in the center of the CE. Two others are positioned between the CE and the guard.

To obtain readings Sensor A must be placed on a thin sponge 7-inches in diameter. Prior to placing, the sponge is moistened with 'grocery store' purchased distilled water.

3.2.1.3 Sensor B

Sensor B is used for mapping corrosion potentials and/or concrete resistivity. The photo on the left in Figure 3.4 shows Sensor B with the sponge cap that must be in place to conduct testing. On the right the end of Sensor B is shown without the sponge cap. The stainless steel counter electrode is used to obtain resistivity measurements. At the center of the stainless CE is a fritted rod that connects the internal reference electrode with the sponge. Prior to using Sensor B, the sponge must be moistened.

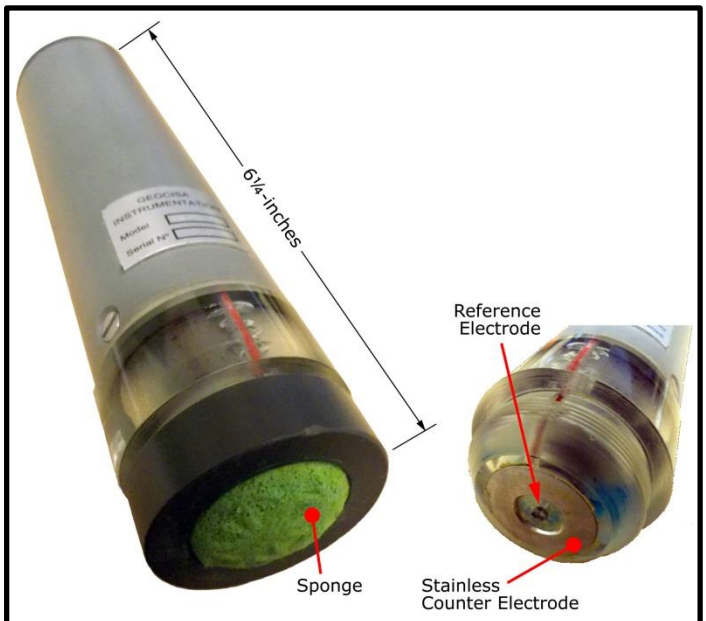

Figure 3.4: Sensor B

3.2.1.4 Sensor C

Sensor C is used for measurements in submerged or very wet locations and was not investigated as part of this work.

3.2.1.5 Dummy Cell

The Gecor Dummy Cell contains an electric circuit that simulates the corrosion behavior of steel embedded in concrete. Figure 3.5 shows the dummy cell that is used to test the Gecor 9 instrument. The dummy cell has two switches. The first allows switching between simulated active and passive corrosion behavior. The second switch allows switching between simulations of atmospheric exposed concrete (aerial) and submerged (or very damp) concrete. On the top of the dummy are two connections. One is for the cylindrical pin connector terminated cable normally connected to

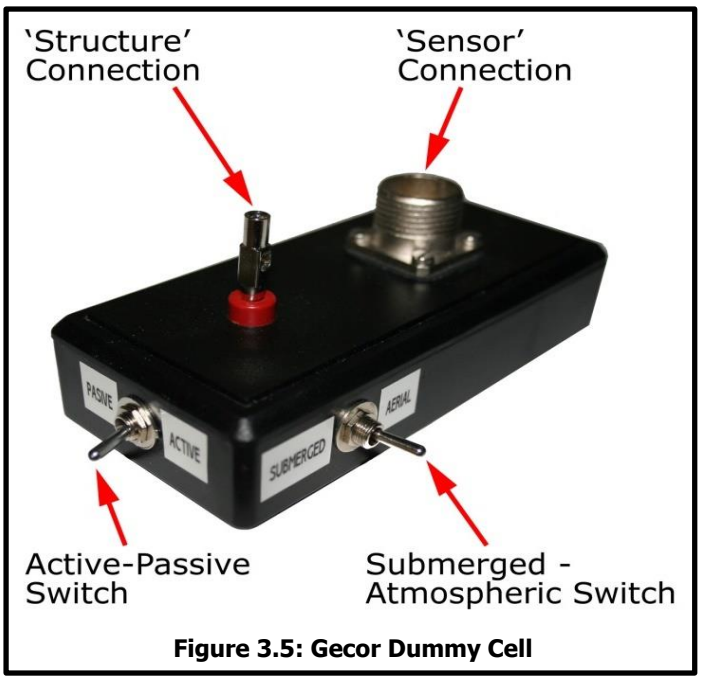

Figure 3.5: Gecor Dummy Cell

Sensor A or B. The other connection is for the meter cable that is normally connected to the structure (the rebar).

On each day we conducted testing with the Gecor, we used the dummy cell prior to that testing to verify proper performance. We found the dummy cell to work well and detailed instructions on its use may be found in Appendix G.

3.2.2 Corrosion Rate Testing

Linear behavior defined in Stern-Geary Equation (Eqn 1) is generally valid for the range of from ±5 to ±20mv from the free, or "open circuit" potential of the steel reinforcement. R_p is the slope, $\Delta E/\Delta i$, of the linear plot of the rebar potential versus current applied near the free corrosion potential. R_p measurements may be taken many ways.

This area of linear behavior, known as the Tafel region, can be expressed as:

$$x = \frac{k \times \mathrm{B}}{R_p \times A} \qquad \textbf{Eqn 4}$$

Where **x** = corrosion rate (μm/yr), **k** is a constant (11.53×10^{-3}), **A** is the surface area of steel being polarized, and **B** and $\boldsymbol{R_p}$ are as before. With conditions as shown in Figure 2.11, the concrete resistivity and depth of cover can produce a wide variation in the surface area of the steel being polarized and thus would introduce a non-trivial error in making calculations of the actual corrosion rate of embedded reinforcement were it not for the Gecor's GE.

As discussed above, the two most common approaches are galvanostatic and potentiostatic. Both approaches to measure R_p require a power supply to apply current between the CE and the WE. The Gecor 9 operates in the galvanostatic mode and assumes that the constant B has a value of 26 mV. The tests take 4-10 minutes per location after the lift is in place. The Gecor reports the corrosion rate, $i_{corr} = B/R_p$, in μA/cm². Equation 4 can be used to convert that value to section loss per year if that is desired.

The Gecor 9 employs an advanced modulated confinement technique to reduce attenuation of the applied current. As discussed previously (see Figure 2.13 and adjacent discussion), this works by applying a small current to the rebar and measuring the change in potentials with two auxiliary reference electrodes. The change in the potentials measured with these two electrodes is used to control the output of the GE. Detailed instructions on conducting corrosion rate testing can be found in Appendix G, the Gecor Instruction Manual.

3.2.2.1 Passivity Verification Testing

One of the key tests the Gecor 9 provides is the ability to evaluate the performance of CP systems without having to interrupt the applied current and/or wait for depolarization that can take weeks or months. As previously discussed, the Gecor uses an EIS-like method to perform PVT evaluation of CP effectiveness. The PVT procedure applies a signal with an amplitude of ± 100 mV at five fixed frequencies of 100, 10, 1.0, 0.1, and 0.01 Hz (*Martinez, 2008*). Using five fixed frequencies from the low end of the spectra reduces the time required to perform the test. As with the DC-based

corrosion rate testing discussed in 3.2.1.6, the AC-based PVT employs the GE to confine the applied current. The PVT test takes 12-15 minutes per location after the lift is in place.

Since the PVT evaluation of the CP system applies AC signals and measures AC-based behavior, the IR-derived voltages produced by the current output from the DC rectifiers is not a problem. The five low frequencies were selected because it is in this range that distinct changes occur in the observed phase angle between potential and current maxima. The Gecor 9 uses this displacement of the frequency where the maximum phase angle appears to provide qualitative evaluation of the condition of the rebar under CP (*Martinez, 2008*). With the Gecor these are identified as ***Well Protected***, ***Protected***, and ***Non Protected***. These three qualitative indications of the effectiveness of the CP system provide the operator clear and meaningful information and guidance on the proper settings required to provide protection.

3.2.2.2 Corrosion Potential and Resistivity Measurement and Mapping

The Gecor 9 can collect rebar potential readings using Sensor B. Concurrent with measurement of the potentials, the Gecor can also measures concrete resistivity using the disk method originated by Newman (*Newman, 1996*). This procedure estimates the resistivity of an electrolyte by measuring the resistance between a small disc placed on the surface of the electrolyte and a much larger electrode placed at infinity. The equation used is:

$$\rho = 2\,a\,R \qquad \textbf{Eqn 5}$$

where $\boldsymbol{\rho}$ is the resistivity of the electrolyte, $\boldsymbol{a}$ is the diameter of the small disc, and $\boldsymbol{R}$ is the resistance. This is, after a fashion, a variation on the 2-electrode type of resistivity measurement common in corrosion engineering.

The Gecor 9 Sensor B has a 20 mm (0.79-inch) counter electrode that is used for the 'small disc.' Actually this counter electrode is shaped more like a common washer (see Figure 3.4). The Gecor obtains the resistance measurement by using a galvanostatic pulse (*Andrade, 2007*). The resistivity is reported in KΩ and is the average of four tests.

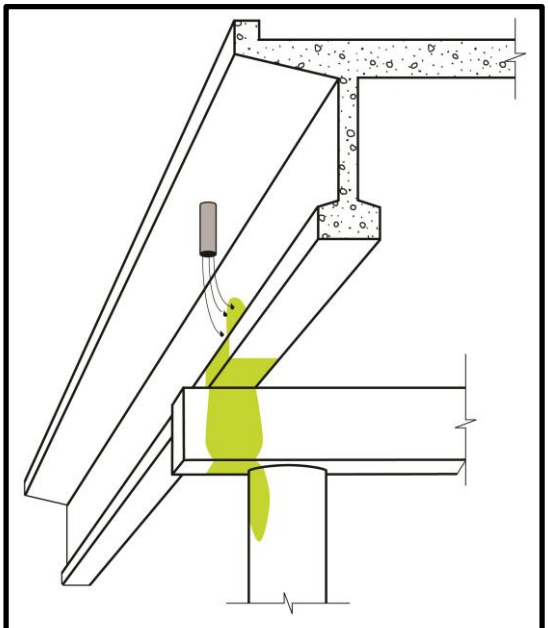

Figure 3.6: Aspirating Scupper

The applicability of the disk method to measure concrete resistivity was investigated by Feliu et al (*Feliu, 1996*) who found that it provided values similar to those obtained using the Wenner 4-pin technique (*Wenner, 1916*). Ideally these measurements should not be made directly over the reinforcement. Rather they, like other 2- and 4-pin measurements, should be obtained at a distance from the rebar, say in the middle of the grid formed by the intersecting rebars. Although these tests only take a few seconds to conduct, the requirement to locate and mark the rebar locations prior to mapping concrete resistivity creates an obvious labor demand. That said, limited mapping might be worthwhile if there are areas where the concrete resistivity

might be skewed, such as in areas where scuppers drain or aspirate on substructure elements as shown in Figure 3.6.

Since each Gecor 9 Sensor B reading took our team members two to five seconds, it is our opinion that for surveying relatively large areas and subsequent mapping of the rebar potential data, the Gecor 9 is much more time consuming that using the Proseq Canin. The wheeled electrode with an integral shaft-encoder that takes readings at programmable distances was far more efficient that chalking a grid and taking readings one at a time. The Canin does not measure resistivity, so no comparison can be drawn between it and the Gecor on obtaining those readings. That said, since it is necessary for accurate measurements to map the location of the nearest mat of rebar, wholesale resistivity mapping would be labor intensive.

3.2.3 Preparing the Test Locations

3.2.3.1 Preparing the Concrete

Although construction work at Coos Bay was still in progress installing the TS zinc CP systems, all of the zones the team was to inspect already had the metallized zinc anode applied prior to our conducting the corrosion rate testing and evaluation of the Gecor 9.

Figure 3.7: Using Needle Gun to Remove Zinc

To conduct the testing, the zinc anode coating needed to be removed at each test location. Several methods to do this were considered by the research team including grinding and the use of needle gun scalers. The research team discussed the preparation with the access subcontractor who has decades of experience in the application of TS zinc anode systems to reinforced concrete structures. The subcontractor recommended that we would have better success with needle scalers as it was their experience that grinders would keep smearing the zinc coating in the areas where we were trying to remove it. Figure 3.7 shows a person using a pneumatic needle gun to remove zinc coating from a test site on the top of an arch.

The research plan included obtaining test measurements with both the type A and type B sensors. Since the sensor-concrete contact area of the Gecor Sensor A is much larger than Sensor B, it was used as the 'template' for the zinc removal. Sensor A has diameter of 7 inches. Because the zinc coating is the CP anode we wanted to minimize the foot print where we would remove zinc. In addition to the size of the area where the zinc coating was removed, we needed to evaluate how free of metallic zinc the surface needed to be to allow the team to obtain stable measurements with the several Gecor sensors.

The test went as follows: a damp sponge is placed between the face of Sensor A and the concrete. If the area cleaned of zinc is too small or the sponge is too wet and water wets the surrounding zinc, the ability of the Gecor to control the GE and obtain accurate readings is compromised. As there is not a body of information on conducting this type of testing on TS zinc CP systems, defining the geometry of the test area and 'how clean was clean enough' was an iterative process.

Sometimes, but not always, shorting the Gecor sensor to the zinc would generate error routines and post messages regarding problems in obtaining a stable reading. However, the error routines did not provide complete protection from issues related to producing a short circuit between the GE and the surrounding zinc. Sometimes when a short occurred the Gecor would obtain and record a reading that would be seen as erroneous and discounted after review by an individual who is well experienced in corrosion rate testing of steel in concrete.

Figure 3.8a shows an early test area after the zinc had been removed and an LPR corrosion rate test had been run using the Gecor Sensor A. This attempt tried to provide a half-inch clearance around the 7-inch diameter sensor. The dark concrete within the area where the zinc was removed is from the damp sponge placed between the concrete and Sensor A. Figure 3.8b shows a close-up of the area and the presence of zinc on the surface can easily be seen. The reading obtained during this test was not sensible.

Figure 3.8a: Early Gecor Test Area

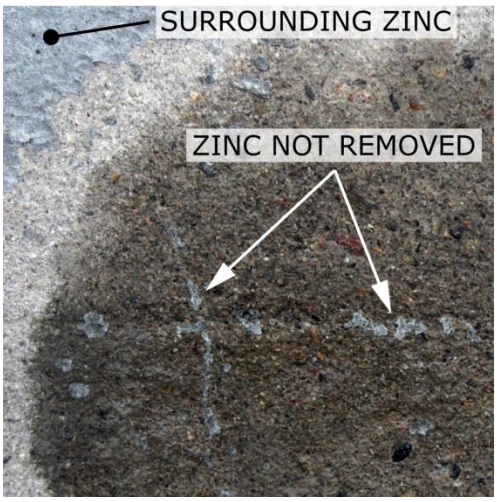

Figure 3.8b: Test Area Close-Up

We eventually settled on cleaning areas that were about 8.5 to 9 inches in diameter. We also carefully checked the surface to ensure that zinc was not left behind in recesses as can be seen in Figure 3.8b. Also, after the needle gun cleaning was complete we performed a thorough blow-down with oil-free compressed air to lift zinc dust from pores and bug holes in the concrete.

3.2.3.2 Adding Anchors

As the Coos Bay Bridge CP system was installed on the deck soffit, beams, and bridge substructure, many of the test locations required the Gecor sensors be placed against a vertical surface or overhead. Although neither of the sensors used in this work are particularly heavy,

variations in pressure when trying to perform the tests while holding the sensor in place by hand were not successful. In addition to hand movement during a test that might take up to 15 minutes, the wind can produce vibrations that make obtaining stable readings difficult.

In order to avoid moving the Gecor sensor during measurements, eye bolts were installed as shown in Figure 3.9. Short bungee cords fitted with hooks were used to secure Sensor A to the concrete surface at both vertical and overhead test sites. Care was taken to avoid shorting the anchors to the zinc, as that would turn the steel into an impressed current anode and they would corrode and possibly crack the concrete.

Figure 3.9: Sensor A during a Test

Over multiple visits we found the eye bolts and bungee cords worked very well to securely hold the Gecor sensor in place.

3.2.3.3 Rebar Location

When conducting LPR corrosion rate testing and PVT evaluation of CP system performance, the Gecor 9 the sensor should be centered over the rebar being evaluated. When measuring concrete resistivity, the manufacturer recommends that Sensor B be placed at a distance from the rebar rather than directly over it. This is especially true where concrete cover is shallow. This will be discussed in greater detail in Section 4.

Almost all of the testing performed at Coos Bay was performed after the zones had been sprayed with zinc. The presence of the zinc coating prevents rebar locators from being able to locate the reinforcement. For locations near test wells and rebar bonds, we could make a reasonable estimate to at least one rebar location. In other areas, it was only after the zinc was removed from the concrete to provide the measurement footprint that we were able to locate rebar. As wholesale removal of zinc would be damaging to the CP systems and was not part of the research plan, at a number of Coos Bay test locations we were not able to center Sensor A directly over the rebar. Because the diameter of Sensor B is only about 1.5 inches, compared to 7 inches for Sensor A, we were able to place that at a distance from the rebar as is recommended by the manufacturer.

For future work, it would be much simpler to determine the rebar locations and depth of concrete cover prior to metallizing. Then the test areas could be masked before application of the zinc coating. This would also be much less time consuming than removing the zinc coating with a needle gun.

3.2.4 Access

3.2.4.1 Conde McCullough Bridge, Coos Bay

At Coos Bay a 120' basket lift and a 160' crane fitted with a bucket were employed to gain access to most of the test locations. Some locations low on the arches and piers could be accessed on foot or with a ladder. Figures 3.10a and 3.10b show the team members using the crane and lift respectively.

Figure 3.10a: Crane Access

Figure 3.10b: Lift Access

Generally speaking, use of the basket lift allowed the inspectors to work more efficiently. Although the crane had a longer boom, only one person could be in the bucket at a time, and since space within the bucket was very limited even mundane tasks, such as reaching down to the bottom of the bucket to get the distilled water jug to moisten the sponge used with the sensor while not dropping or getting water on the Gecor was problematic.

Moving the access equipment at Coos Bay also presented challenges. Note in Figure 3.10a that the support pads of the crane are set on timber. The southernmost two arches, Spans 13 and 14, reach over designated wetlands. The team had to exercise special care when inspecting in this area so that our access equipment did not damage the soft soil. The presence of the wetlands and need to move and place timbers for each access rig setup considerably slowed inspection efforts in that area. Accordingly, we tried to cluster test locations so that more than one test site could be accessed from a single lift rig setup.

Some of the inspection work on Span 12 required a flagger, as that span crosses a public road. Having to set-up, move, and take down lane closure warning signs also slowed inspection work.

Although Spans 11 and 10 were within non-public access boundaries of the construction site and did not have wetland or flagger requirements, the staging and storage of equipment under the bridge did create some impediments to being able to quickly move the access equipment from one set-up location to the next.

At Coos Bay the wind typically increases in the afternoon. Early in the initial inspection, the wind became sufficiently strong that we would have to cease work from the lift and crane well before the end of the 'normal' workday. Therefore, to maximize our inspection time, we changed our shift schedule and started our inspection work at 4:00 AM.

3.2.4.2 Lint Creek Bridge, Waldport

Access to Lint Creek was provided by an under bridge inspection truck. The platform provided good access to the areas inspected. Given the elevation of the bottom of the stringers was less than 15 feet above mean lower low water and the clearance required by the platform, we had to make sure our scheduling avoided higher tides that could flood the platform hydraulics and wiring.

Lint Creek is a two-lane bridge, and that fact required closing the westbound lane in order to be able to park the platform truck on the bridge in locations such that our team could access the underside of the bridge where the CP system was installed. With significant tourist traffic demands in this area, it was incumbent on the team to schedule the Lint Creek inspections well in advance of the actual under bridge work.

3.2.4.3 Yaquina Bay Bridge, Newport

Access at this location was easiest of the three locations. We were able to reach the areas that needed to be inspected with the 120' basket lift. Further, there were few encumbrances to moving the lift from one location to the next.

4.0 FIELD TESTING RESULTS

4.1 ICCP SURVEY – COOS BAY BRIDGE

4.1.1 Overview

Part of this investigation included evaluation of several operation modes for CP systems that were being installed on the south approach spans of the Coos Bay Bridge. The CP systems protect atmospherically-exposed conventionally reinforced concrete bridge spans. The southernmost spans are reinforced concrete deck girder (RCDG) simple spans. The RCDG spans are followed by longer deck arch spans, which terminate at the main steel spans. Figure 4.1 shows an elevation view of these spans.

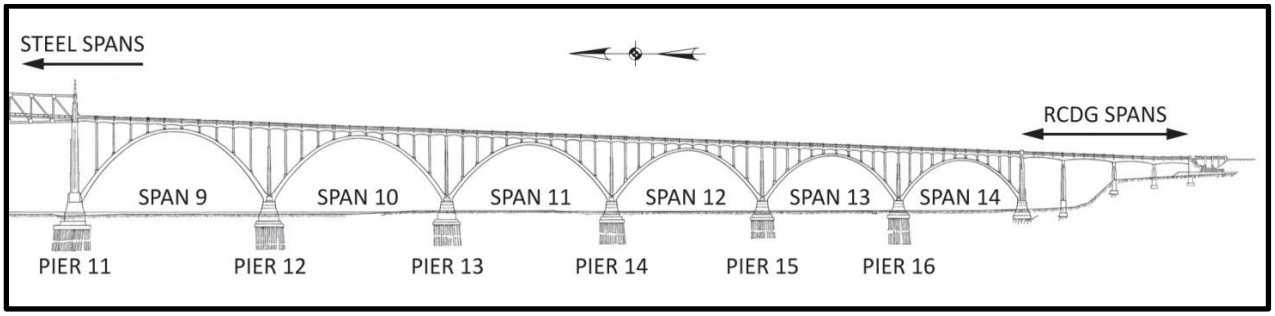

Figure 4.1: Coos Bay Bridge South Approach Spans

This system is broken into 37 discrete zones, which protect both the superstructure and the substructure of the spans. The physical elements that comprise the south approach vary in structural function, reinforcement density, depth of concrete cover, general exposure to the weather, and elevation. The discrete zones allow for these variations. Employing multiple zones also improves constructability and construction quality control. The zone approach also improves the ability to adjust and operate the system.

The TS zinc coating applied to the concrete surface operates as a distributed anode. The TS zinc coating is connected to the positive terminal of a rectifier that powers the system through what is known as a primary anode. A primary anode is a piece of brass set in a recess cut into the concrete in such a manner so as to insure the outer brass surface is flush with the surrounding concrete surface. The primary anode is installed before the zinc coating is applied. Spraying the zinc over the brass surface shorts the distributed zinc to the primary anode. A wire is then connected to the primary anode and run to the rectifier. This connection to the primary anode also is connected to the distributed zinc anode.

Figure 4.2 shows the installation steps of a primary anode through spraying with zinc.

FIGURE 4.2a: Cut Recess for Primary

Figure 4.2b: Epoxy Primary in Place

Figure 4.2c: Primary Installed

Figure 4.2d: Apply TS Zinc

A second cable connection runs between the negative terminal of the rectifier and the steel reinforcement embedded in the concrete. The concrete itself completes the electrical circuit as is shown in Figure 2.16a.

Each zone has a minimum of two primary anodes and two connections to the reinforcement. Two permanent reference electrodes are also located in each zone. Each reference also includes a connection to the reinforcement and a test well that afforded direct contact to concrete that was not covered with the TS zinc distributed anode. Having multiple access points to reinforcement connections, primary anode connections, and embedded reference/test well locations was a tremendous asset to this work's field investigations and testing.

Figure 4.3 shows a typical test well location at the Coos Bay Bridge. Starting at the bottom is the test well. The location of the embedded rebar is shown in the figure as a dashed green line.

To install a test well the contractor first accurately locates a rebar. A cylindrical excavation is then made in the concrete on one side of that rebar, in this case to the left of the rebar at the bottom of the photo. A short section of threaded PVC is fitted to the hole and secured with epoxy. This pipe is fitted with a PVC cap that can be removed to gain access to concrete that is not coated with TS zinc. Absent the zinc coating it is then possible to obtain readings of the embedded steel bar using a portable reference electrode set on concrete at the bottom of the well. The bottom of the well is set to the approximate depth of the adjacent rebar.

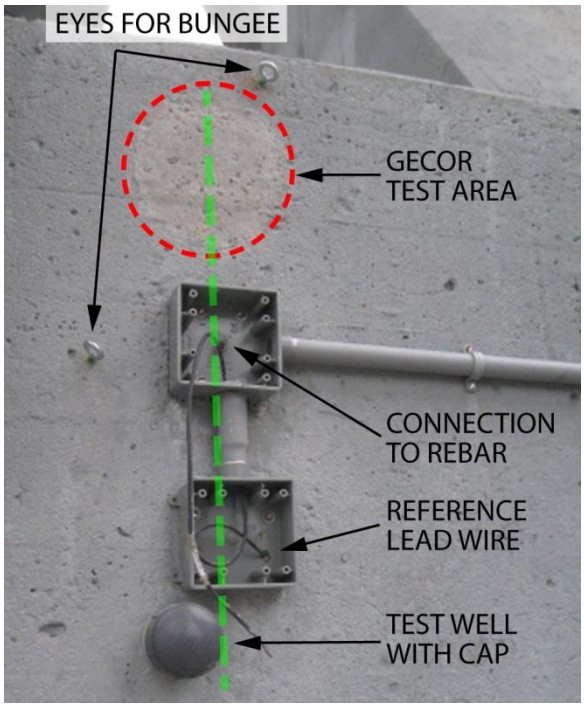

Figure 4.3: Typical Zone Test Well Location

A second excavation is made on the opposite side of the rebar and a permanent reference electrode is embedded at this location (located beneath the square J-box to the right of the rebar and above the test well). When making the excavations for the test well and the permanent reference electrode care is required that the work does not expose the adjacent rebar. A third excavation, above at center in the photo, is where a connection is made to the rebar.

These test wells are typically at locations identified through potential mapping as being the most anodic sites within the zone. Sometimes other factors are used to ensure these test sites reflect other elements of concern. For example, this location at the base of a pier is at the greatest linear distance from the primary anode and thus helps to evaluate attenuation of the CP current.

4.1.2 Selection of Test Sites

For each zone, six locations were selected for testing using the Gecor 9. A number of factors were considered in the selection process including:

- Distance from primary anode to evaluate attenuation of CP current
- Areas with patches and areas with original concrete
- Areas exposed to the weather and areas shielded from the weather
- Areas exposed to discharge from deck drains
- Areas with differing structural activity (i.e., members in compression and others that flex)

The rectifiers connect to the TS zinc anode at a limited number of primary anodes. From the primary anode connection the current flows into the zinc coating and across the concrete surface.

How far a distance from those primary anodes the current flows may affect observed local CP current density. Although zinc is a conductive metal, it is present on the concrete surface as a thin (10 mil) coating. Like copper wire, the resistance in the CP circuit will increase with distance from a primary anode. Figure 4.4 shows a stylized sketch of this behavior.

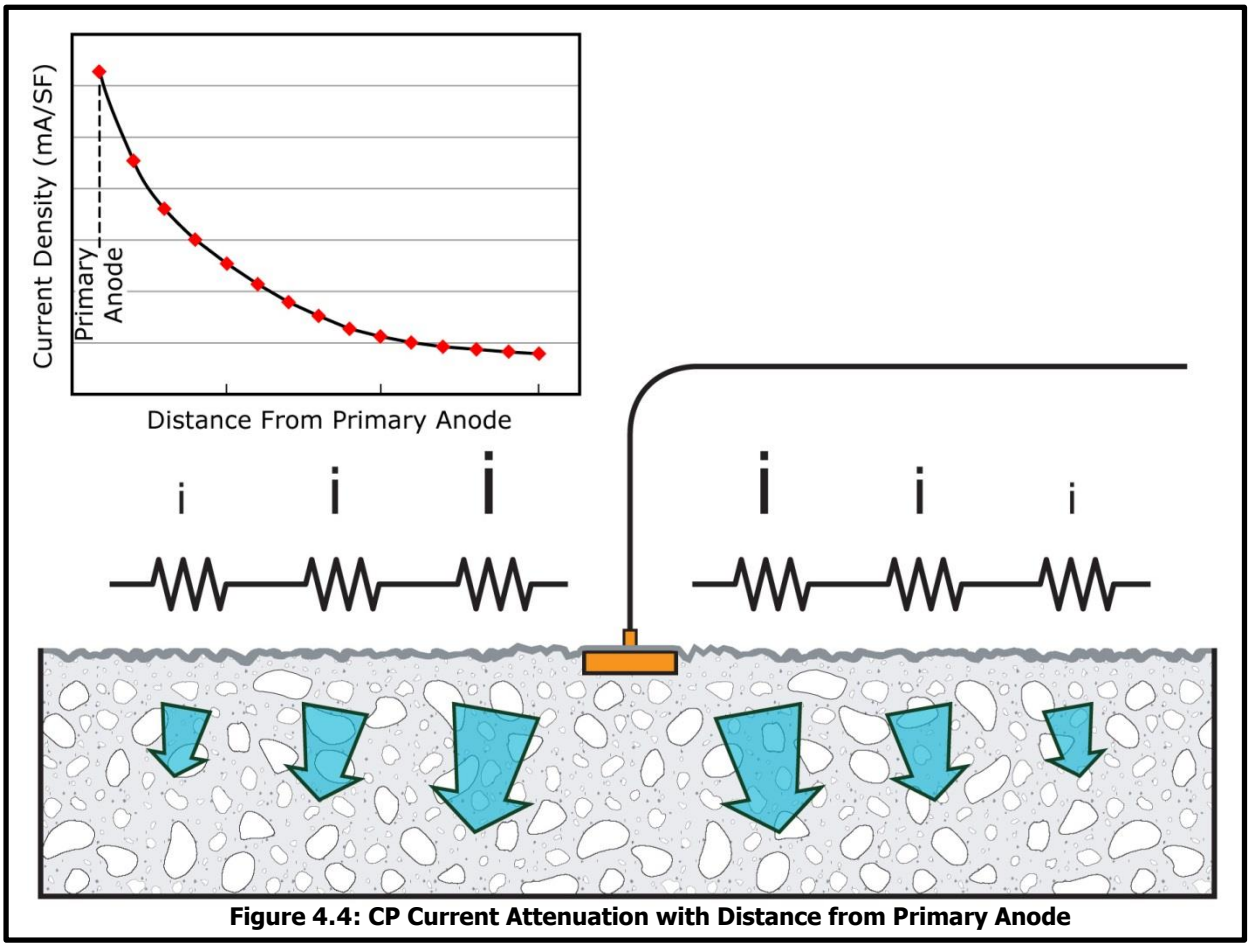

Figure 4.4: CP Current Attenuation with Distance from Primary Anode

In the upper left corner of Figure 4.4 is plot of idealized attenuation of CP current as a function of distance from the primary anode. Although variations in depth of concrete cover, exposure to rain or other source, and concrete (patch vs. original) will skew the attenuation of CP current from the ideal, the selection of test locations looked to include locations that were at varying distance from primary anodes.

The patch material is not identical to the original concrete, so an effort was made to include in the test sites both patched and original concrete. Following this concept of variation, test locations include areas boldly exposed to weather and/or deck drain water as well as locations that see little if any rainfall or other direct wetting other than from dew and fog droplets.

As mentioned previously, twenty-one zones were tested. For operation purposes fourteen of the zones were to be operated in constant current (CC) mode, and seven in constant voltage (CV). In each zone six test locations were created for 126 total test locations. Appendix A provides drawings that show the location of all of the Coos Bay Gecor tests sites.

Separate zones protect decks, sidewalks, piers, and arches. The manner in which the Coos Bay Bridge zones were configured contributes significantly in being able to see if the concrete being in compression or in flexure contributes to the observed behavior of the CP systems. Table 4.1 shows how the CC and CV rectifier operating mode was distributed between the sidewalk zones, deck & beam zones, the arch and columns zones, and the pier zones.

Table 4.1: Rectifier Operating Modes

ITEM	No. ZONES		
	CV	CC	SUB
Sidewalks	1	3	4
Deck & Beams	2	2	4
Total Flexural:	3	5	8
Arches & Columns	2	6	8
Piers	2	3	5
Total Compressive:	4	9	13
Total Entire Bridge:	7	14	21

Seven nominal current outputs were employed as part of this work. These outputs ranged from 0.050 to 0.200 mA/SF in increments of 0.025 mA/SF. The output of 0.200 mA/SF is the traditional nominal current density employed by ODOT in most of their ICCP zones.

Table 4.2 shows the allocation of these seven nominal outputs.

Table 4.2: Output Allocation by Element and Rectifier Operating Mode

ITEM	ZONE CURRENT DENSITY (mA/SF)						
	0.050	0.075	0.100	0.125	0.150	0.175	0.200
Sidewalks			CC		CV	CC	CC
Deck & Beams	CV	CC		CV	CC		
Arches & Columns	2 CC	CC	CV	CC	CC	CC	CV
Piers		CV	CC	CC		CV	CC

In CC mode, the nominal surface area of the zone is multiplied by the desired current density to provide the current output to which the rectifier will be set. For example, Pier 13, Zone 11, has a nominal surface are of 4,755 SF. Zone 11 was selected to be operated at a current density of 0.200 mA/SF. Multiplying the area of Zone 11 by the desired current density produced a desired output of 0.95 amps, so the Zone 11 rectifier was set to provide CP current at that level.

In CV mode, the idea is similar. Zone 22, the west arch of Span 22, was selected to operate in CV mode at an initial current density of 0.200 mA/SF. The nominal surface area for Zone 22 is 7,402 SF, so by multiplying that area by the desired current density an output of 1.48 amps was required. To operate in constant voltage mode the rectifier output voltage was increased until the desired output of 1.48 amps was reached. The system output resistance of TS zinc ICCP systems is known to increase with time (*Covino 2002*). Ohm's Law E = IR, tells us that if the system output voltage remains constant, as it would in CV mode, then the output current will drop as the resistance increases. For that reason, when the CV rectifiers were energized, their voltage was

increased over a period of one to two days to reestablish the desired output. After initial energizing the rectifier voltage was not adjusted.

4.1.3 Obtaining Baseline Data

Prior to energizing the rectifiers, the team collected baseline data on the corrosion condition of the 126 test locations at the Coos Bay Bridge. The results from the pre-energizing survey are presented in Appendix D. The pre-CP data shows that the system being installed is more one that provides cathodic prevention than cathodic protection. Thirty-one percent of the locations exhibited a negligible corrosion current of <0.1 μA/cm². Almost sixty-two percent of the locations exhibited low corrosion currents (0.1 – 0.5 μA/cm²). Just over four percent showed moderate corrosion rates (0.5 – 1.0 μA/cm²), and just over 3 percent showed high corrosion rates (>1.0 μA/cm²).

4.1.4 Energizing the Systems

The rectifiers employed at Coos Bay were capable of operating in either constant current or constant voltage mode. Task 2.1 was to energize 14 zones in constant current mode and Task 2.2 was to energize 7 zones in constant voltage. Seven output current densities were employed. These were 0.200, 0.175, 0.150, 0.125, 0.100, 0.075, and 0.050 mA/SFT with one constant voltage zone at each current density and two constant current zones set at each current density. Further, we attempted to distribute the several structural elements (i.e., decks, sidewalks, arches, columns, and piers) representatively between our allocations for those zones operating in constant current and voltage modes.

4.1.4.1 Overview of Changes Resulting from Applying Cathodic Protection

Passing an electrical charge in the proper direction across the reinforcement-concrete interface is what the CP system does to reduce corrosion to an insignificant rate. Once the protection level is reached, passing more current to the rebar provides no additional benefit. The passage of electrical current also will reduce the chloride content and increase the pH of the cement surrounding the reinforcement. With time, this change in chemistry will return the reinforcement to a passivating environment and the amount of CP current needed to sustain that environment will be significantly less than when the reinforcement was corroding. In fact, with proper monitoring, intermittent CP would be possible where the current is interrupted and only applied at intervals necessary to sustain the passivating low chloride / high pH environment around the reinforcement (*Cramer, 2005*).

As Covino noted (*Covino, 2002*) when electric charge is passed across the zinc-concrete interface several things occur. These include: 1) zinc will convert from metallic to ionic form; 2) zinc ions will engage in secondary mineralization replacing calcium ions in portland cement hydration products; 3) the secondary mineralization increases the interfacial electrical resistance; 4) at higher current densities, acidification can occur producing a reaction zone with substantially reduced calcium content. In short the passage of electric charge at the anode interface consumes the TS zinc coating and produces changes in the cement that do not improve the operation of the CP system.

In Section 2.2.4 we discussed Evans diagrams showing the behavior of corroding and passive steel. Figure 4.5 shows a generalized Evans Diagram for ICCP applied to steel in a neutral or alkaline environment (*Cramer, 2003*). Given the chemistry that occurs at the TS Zinc anode-concrete interface we would expect this to initially be an alkaline environment that might with time and charge passage move towards a more pH neutral regime. Note that two anodic and cathodic reactions are shown. The two anodic reactions are:

$$4OH^- \rightarrow O_2 + 2H_2O + 4e^-$$
$$Fe \rightarrow Fe^{2+} + 2e^-$$

And the two cathodic reactions are:

$$O_2 + 2H_2O + 4e^- \rightarrow 4OH^-$$
$$2H_2O + 2e^- \rightarrow H_2 + 2OH^-$$

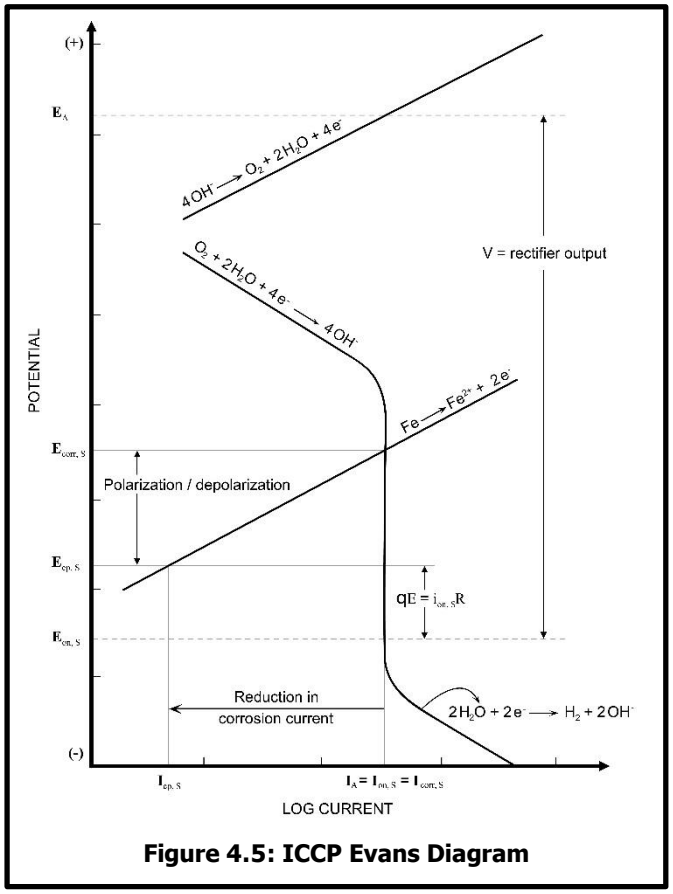

Figure 4.5: ICCP Evans Diagram

The application of CP polarizes the iron in a negative direction and hence reduces the iron corrosion rate as shown in Figure 4.5. With routine CP voltages applied to the TS zinc anode exposed to a basic to neutral pH environment, the anodic reaction would be where four hydroxyl ions oxidize to water and oxygen. Although with time this consumption of alkaline hydroxyl ions at the anode-concrete surface can reduce the local pH, the vast quantity of hydroxyl ions in the surrounding concrete can buffer this process provided the current densities and/or voltages are not too high.

Hence, the ideal CP system will reduce the rebar corrosion rate to a level that is below engineering significance with the fewest possible coulombs. Toward that goal, the two rectifier operating modes of constant current and constant voltage afford differing benefits.

Seasonal variations in concrete moisture content and temperature will affect the CP system electrical resistance (*Covino, 2002*). Further, Covino and his coworkers noted that these effects become additive, and with system aging, changes at the anode-concrete interface dominate.

4.1.4.2 Constant Current Mode

When operating in constant current a specified current density is continually provided. Even with increases in electrical resistance at the anode-concrete interface, when operating in constant current mode the rectifier provides the preset output. However, the CP current demands for each zone will vary with changing temperature and moisture conditions over the course of the year. In the winter time the colder temperatures will reduce the rate of chemical reactions and hence less current is required to maintain passivation. Also, during late summer the concrete dries out and its electrical resistance becomes much greater. From Ohm's law this increase in resistance will

reduce the current necessary to sustain reinforcement passivation. So when the rectifier output is set to provide the necessary current output to mitigate rebar corrosion in the spring, early summer, and fall, it most likely is providing too much current for conditions in the winter and late summer and hence consuming more TS zinc than is required and excessively increasing electrical resistivity at the anode-concrete interface.

Following are the zones energized to operate in constant current mode:

Table 4.3: Coos Bay Constant Current Zones

CP Zone	Spans	Bents	Bottom of sidewalk	Sidewal Barckets and Beams	Bottom of Deck	Longitudianl Deck Girders	Transverse Deck Beam	Arches	Columns	Piers & Bents	Area	Set Current	Set Voltage (panel / portable)	Mode	Current Density
11		Pier 13								●	4,755	0.95 A	/	CC	0.200 mA/SFT
12	Arch Span 11							●	●		9,307	0.47 A	/	CC	0.050 mA/SFT
13	Arch Span 11							●	●		9,307	1.40 A	/	CC	0.150 mA/SFT
14	Arch Span 11		●	●							4,587	0.46 A	/	CC	0.100 mA/SFT
17	Arch Span 12							●	●		8,286	0.62 A	/	CC	0.075 mA/SFT
19	Arch Span 12		●	●							4,264	0.75 A	/	CC	0.175 mA/SFT
20	Arch Span 12				●	●	●				10,380	0.78 A	/	CC	0.075 mA/SFT
21		Pier 15								●	3,797	0.47 A	/	CC	0.125 mA/SFT
23	Arch Span 13							●	●		7,402	0.93 A	/	CC	0.125 mA/SFT
25	Arch Span 13				●	●	●				9,642	1.45 A	/	CC	0.150 mA/SFT
26		Pier 16								●	3,366	0.34 A	/	CC	0.100 mA/SFT
27	Arch Span 14							●	●		6,793	0.34 A	/	CC	0.050 mA/SFT
28	Arch Span 14							●	●		6,793	1.19 A	/	CC	0.175 mA/SFT
29	Arch Span 14		●	●							3,667	0.73 A	/	CC	0.200 mA/SFT
											215,367				

4.1.4.3 Constant Voltage Mode

When operating in a constant voltage mode, changes in circuit resistance will produce inversely proportional changes in current output. If the resistance of the bulk concrete or zinc-concrete interface goes up, then the current output will go down. As opposed to constant current operation, the current output in constant voltage mode will change with seasonal variance in CP system resistance. For example, in constant voltage mode, when the concrete dries during the summer the resulting increase in concrete resistivity will reduce the CP. In deference to the cumulative effects of CP charge passage, as part of initial energizing we increased the voltage setting of each of the constant voltage mode systems in response to the increase in circuit resistance for two days following the initial energizing. A similar reduction in output would occur in the winter when cold temperatures can produce higher resistance. In the spring and fall rainfall and moderate temperatures combine to produce a relatively low concrete resistivity, which results in increased current output that then can address the more corrosive conditions.

In follow-up visits, early increases in circuit resistance suggest that a longer period for adjusting the constant voltage output would be beneficial. Although we did not formally evaluate this effect as part of this work, from what we saw here and what we have seen in other TS zinc and carbon paint ICCP systems, perhaps two to four weeks would be a more appropriate adjustment period to allow for early aging effects that increase the CP circuit resistance.

Following are the zones energized to operate in constant voltage mode:

Table 4.4: Coos Bay Constant Voltage Zones

CP Zone	Spans	Bents	Bottom of sidewalk	Sidewal Barckets and Beams	Bottom of Deck	Longitudianl Deck Girders	Transverse Deck Beam	Arches	Columns	Piers & Bents	Area	Set Current (in red inial current for CV)	Set Voltage (panel / portable)	Mode	Current Density
15	Arch Span 11				●	●	●				11,124	1.39 A	/	CV	0.125 mA/SFT
16		Pier 14								●	4,177	0.73 A	/	CV	0.175 mA/SFT
18	Arch Span 12							●	●		8,286	0.83 A	/	CV	0.100 mA/SFT
22	Arch Span 13							●	●		7,402	1.48 A	/	CV	0.200 mA/SFT
24	Arch Span 13		●	●							3,943	0.59 A	/	CV	0.150 mA/SFT
30	Arch Span 14				●	●	●				8,948	0.45 A	/	CV	0.050 mA/SFT
31		Pier 17								●	4,409	0.33 A	/	CV	0.075 mA/SFT
											171,310				

4.1.5 Current Attenuation Testing

For larger structures with distributed anode systems, current attenuation of the anode can be a significant concern. In order to address this issue, multiple anode connections were made in each zone. However, there were still several places such as along arches and up the longer columns where the anode connection was a significant distance from the end of the zinc. In order to test the extent of the attenuation along these areas, potentials were plotted along a linear path from the anode connection to the more remote sections on three different zones. Potentials were taken with the CP system on in order to measure the zinc under load.

The first zone tested was along the face of a pier, the second was measured along the top of an arch, and the third from up one of the longer columns. For each of these tests, the potential of the zinc varied less than 20mV from the anode connection to the extents of the testing. This shows that the zinc remote from anode connections was not receiving significantly less current than at locations closer to the primary anodes.

4.1.6 Gecor 9 Testing

One of the key features of the Gecor 9 is its ability to rate the level of CP protection without having to interrupt the output of the CP current. As discussed above in 3.2.1.7, and elsewhere, this is because the Gecor evaluates rebar passivity using the AC-based PVT technique.

4.1.6.1 Gecor Data

Appendix D provides a detailed breakdown by zone of the 126 test locations. The initial pages present data obtained on the corrosion condition of the rebar at each site prior to the application of CP current. That is followed by a tabular appendix containing basic information including: the span, the structural type, the nominal output, the presence of a test well, if the location was in a drain or joint water runoff area, and other location information. It also includes a summary of data collected during the site visits including: rebar potential at the test site, the zone rectifier output, and the level of protection measured by the Gecor 9.

PVT testing indicated 30% of tested locations had some level of protection in April 2012. By June 2012 that number increased to 48%. However, between the June and September 2012 site visits, rectifier power was lost for several weeks and the system lost polarization. As a result, the

September testing only resulted in 17% of test sites showing protection. Rebar potential readings taken with the PVT testing shows an average rebar potential of -0.288V_{CSE} in April 2012, -0.188V_{CSE} in June 2012, and -0.182V_{CSE} in September 2012.

In addition to analyzing the results by date taken, the PVT testing was also examined by zone type and by whether it was a constant current or constant voltage zone. Over all, constant voltage zones had 30% of test locations with protection, while constant current zones showed 67% protection. Piers averaged 30% protection, decks averaged 31% protection, arches averaged 32% protection, and sidewalk zones test locations averaged 36% with some level of protection.

4.2 GACP SURVEY – LINT CREEK BRIDGE

Lint Creek employs embedded zinc GACP, see Figure 4.6. Interrupting the embedded zinc anodes and monitoring rebar potential decay at multiple locations over time would be tedious. The Gecor 9 PVT testing works well on GACP systems in addition to ICCP systems. In fact, since we did not have to remove zinc from the concrete surface, PVT testing of this application was easier than was the case of the TS zinc ICCP system at Coos Bay. The GACP system at Lint Creek had been in operation prior to our initial inspection, so baseline data was not obtained.

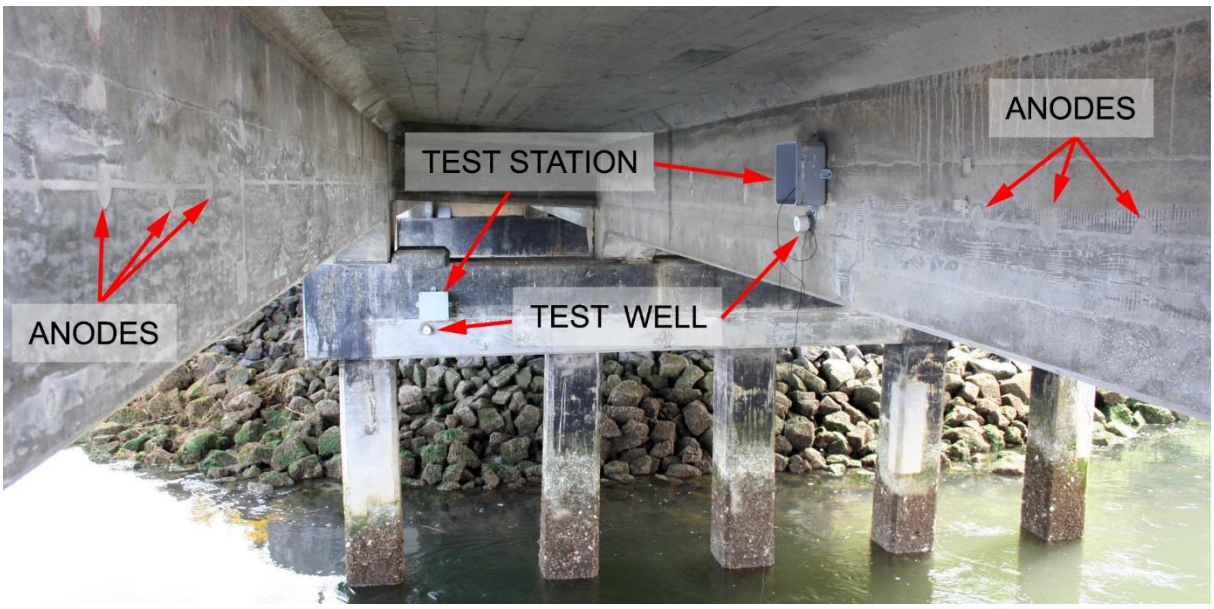

Figure 4.6: Lint Bay GACP System

4.2.1 Gecor 9 Testing

Six locations on the Lint Creek Bridge were tested for passivity using the PVT test on the Gecor. Testing was performed on three separate trips from May of 2011 through September of 2012. Tests were all between galvanic anode locations on the north face of the north most stringer or on the south face of the north fascia beam. A schematic of these locations is located in Appendix B.

PVT results, presented in Appendix E, show a trend of increasing polarization of the reinforcement over the period of the testing. In the initial test, two test locations showed no

protection, three showed moderate protection, and only one was well protected. The following test in June of 2011 had no sites without protection, two were moderately protected, and four well protected. Finally in September 2012, one location was moderately protected and the remaining five showed good protection.

In addition to the PVT testing, the potentials of the steel shifted in the more positive direction over the course of the three tests indicating a shift in the environment to a more alkaline condition, which will help passivate the steel. This data, combined with the PVT testing clearly shows that the reinforcement is receiving good protection at the CP locations.

This behavior follows the concept of return to passivity initially discussed in Section 2.2 Cathodic Protection, and especially Section 2.2.4. The extended application of CP not only protects the embedded reinforcement from corrosion while the current is applied, the application of current is also able to return the environment surrounding the concrete to a passive regime, hence the electropositive shift of reinforcement potentials. Although we did not measure the output of the embedded anodes, it likely will have dropped considerably in response to increase in polarization resistance (see Figure 2.26b) that accompanies this return to passive environments (*Tinnea, 2013*).

4.3 FAILED ZONE SURVEY – YAQUINA BAY BRIDGE

Reports of failing zinc at the Yaquina Bay Bridge led to inclusion of a one-day field investigation of the bridge's south approach as part of this work. In May of 2001 the voltage and currents increased sharply in four south approach zones (*Holcomb, 2002*). The voltage and current outputs observed in 2001 were two to seven times higher than the set points. Those problems were repaired, but subsequent failures in those locations led to outputs 10 times those intended (*Tinnea & Cryer, 2008*). Excessive current density/voltage can severely compromise the bond between the TS zinc and the underlying concrete.

4.3.1 TS Zinc Anode – Interface

4.3.1.1 Zinc-Concrete Interface Chemistry

In a report (*Shi, 2011*) that investigated replacement of TS zinc coatings, Shi et al discussed in part the essential total failure of the coating on the surface of Pier 9 of the Yaquina Bay Bridge. They also mentioned some anodic reactions that might occur at the zinc-concrete interface. Table 4.5 shows several of those reactions and some commentary.

Table 4.5: TS Zinc Anode Interface Reactions

REACTION	COMMENTS
$4OH^- \rightarrow O_2 + 2H_2O + 4e^-$	The loss of pH at the zinc surface depends on the current rate and rate at which hydroxyl ions in surrounding concrete can diffuse to the zinc
$Zn + 2H_2O \rightarrow Zn(OH)_2 + 2H^+ + 2e^-$	By producing hydrogen ions, this reaction will reduce the interface pH with time (*Cramer, 2005*)
$Zn \rightarrow Zn^{2+} + 2e^-$	This is the 'galvanic reaction', but likely occurs during ICCP charge transfer

The zinc ion can then react to produce zinc chloride, zinc hydroxide, and zinc oxide:

$ZnCl_2 + 2OH^- \rightarrow Zn(OH)_2 + 2Cl^-$ $Zn^{2+} + OH^- \rightarrow Zn(OH)_2$	Two paths by which zinc ions precipitate out of solution as relatively insoluble zinc oxide
$Zn(OH)_2 \rightarrow ZnO + H_2O$	Zinc hydroxide can age, dehydrate and form zinc oxide

In some cases the chloride ion can be oxidized to chlorine:

$2Cl^- \rightarrow Cl_2 + 2e^-$	This reaction is not expected with a zinc distributed anode such as the TS zinc used on the main span and south approach at Yaquina Bay Bridge. On the north approach of the Yaquina Bay Bridge, which has a carbon paint distributed anode, this reaction occurs and explains why large chloride build-up is not seen at the carbon paint-concrete interface. (*Broomfield & Tinnea, 1992* ; *Cramer, 2002*)

A number of authors have investigated the species found at the TS zinc-concrete interface looking at both electrochemically aged specimens (*Covino, 1997a*) and specimens obtained from operating ODOT bridges (*Covino, 1997a; Covino, 2002; Cramer, 2005*). They noted zinc hydroxide and zinc oxide at the immediate interface, and that with distance from the zinc and time, secondary mineralization would occur where the zinc would combine with other ions in the matrix such as chloride, sulfate, or carbonate or where the zinc would replace calcium in the cement matrix. With the passage of time, the more chemically stable of these species predominated.

If the current density at the zinc-concrete interface goes beyond the capacity of the surrounding concrete to provide hydroxyl ions, OH^-, and the applied voltage is sufficient then the following reaction can take place:

$$2H_2O_{(l)} \rightarrow O_{2(g)} + 4H^+_{(aq)} + 4e^- \qquad \textbf{Eqn 6}$$

This is known as the electrolysis of water. When this reaction happens at the TS zinc anode-concrete interface there is at once two things occurring that are detrimental to the adhesion of the zinc coating. First, the additional production of acid, can over a short distance, destroy the structural integrity of the underlying cement matrix. Second the production of oxygen gas can produce pressure at the zinc-concrete interface and help to disbond the zinc from the underlying and acid-softened cement, though with the inherent porosity of the TS zinc, gas generation is not likely a major contributor to the loss of adhesion.

4.3.1.2 Impact of Variations in Local Environment

Bridge CP systems are typically broken down into zones that are sized to at once fit the size of the rectifier, performance characteristics of the anode, the geometry of the structure, and the ability to control and provide somewhat uniform CP current output. Figure 4.7 shows the layout of the several CP zones inspected during this inspection, particularly the east side arch Zones 18 and 20, and the south pier Zone 16.

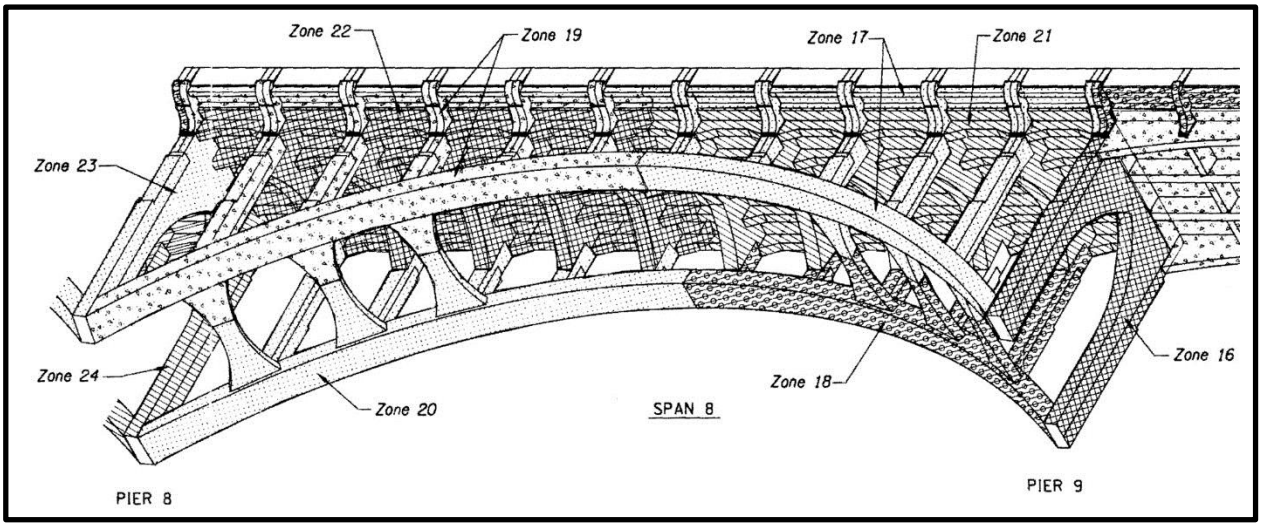

Figure 4.7: Yaquina Bay Bridge Span 8 (*ODOT, 1991*)

Note in Figure 4.7 that one would expect that the top of the arches are more directly exposed to rainfall than are the arch bottoms. Further, the arches would get much greater direct exposure to rainfall than would the underside of the deck. The piers' direct exposure to rain will be higher on the lower portions of the two columns than at the top above the arch. Rainfall affects the CP system output (*Covino, 2002*) by wetting the zinc-concrete interface and lowering the effective circuit resistance. Within a single zone, if all other factors are similar, areas with greater direct rainfall exposure will see a localized increase in CP current output because of that wetting.

Drains that aspirate directly on the concrete surface can cause one area to be wetted much more that relatively close adjacent areas of the same zone. Figure 4.8a is a 2008 photograph that shows

Figure 4.8a: Zone 18, 2008

Figure 4.8b: Zone 18, 2011

an area directly below a scupper that drains directly on the upper surface of the arch in Zone 18

(see Figure 4.7). As can be seen in Figure 4.8b, taken just three years later, weathering has removed a great deal more TS zinc coating (note the area adjacent to the arch column that looks undamaged in 2008 and has spalled in 2011). If there are areas of ponding, the local CP current density can be profoundly higher than nearby locations and damage the anode-concrete interface (see Figure 1.1 and also the discussion in the first paragraph on page 18).

Within a single zone, variations in the depth of concrete cover between the thermal-sprayed zinc anode and the imbedded rebar can produce variations in local current output with the shallower bar getting more current than does its deeper neighbor.

As with all metals, the TS zinc coating has an ohmic component. As discussed in Section 4.1.2, this ohmic component means that as one moves away from the primary anode, the circuit resistance will increase. Figure 2.19b shows chloride salt halos around a primary anode pair on the Cape Creek Bridge. The halos form because of radial current attenuation with distance from the primary anodes at the center of the two square junction boxes. Because they were on the east side of a beam and partially sheltered from direct exposure to rainwater that could wash the salt deposits from the zinc surface, salt deposits developed rather than being washed away. In the piers, distance-from-primary-anode attenuation will be partly mitigated by the fact the fact that lower areas of the pier columns will likely see greater direct rain exposure than do the upper areas where the primary anodes are located and would be expected to have lower anode-to-concrete resistance. Attenuation testing performed as part of this work (see Section 4.1.5) would seem to confirm this combination of factors.

4.3.1.3 TS Zinc Adhesion

ODOT has included adhesion testing of distributed anode coatings as an integral item of CP system installation work going back to the carbon paint system installed on the north approach of the Yaquina Bay Bridge in 1985 and the first TS zinc system they had installed in 1991 on the Cape Creek Bridge. In work funded by ODOT, Covino et al presented initially at NACE CORROSION/1996 (*Covino, 1996*) and then later in Corrosion Journal (*Covino, 1997b*), discussions of the effects of charge passage on the bond of TS zinc to the underlying concrete. The tests employed accelerated electrochemical aging, with TS zinc anode-concrete current densities of 3 mA/ft², approximately 15 times the nominal ODOT current density of 0.2 mA/ft². Their findings included:

- Replacement of calcium by zinc in the zinc-concrete interfacial zone appeared to:
    - Improve TS zinc adhesion to the concrete until approximately 600 kcoul/m² had passed and afterwards the bond strength then decreased
    - Reduced the coating's permeability to water
- The reduction in bond strength would limit the service lives to 29 years
- Increases in output voltage observed at the Cape Creek Bridge field installation matched patterns seen in the lab under accelerated conditions

When the Zone 16 CP system was installed on Pier 9 of the Yaquina Bay Bridge, ODOT required all the adhesion tests must exceed 150 psi. Pier bond strengths averaged 217 psi ±69 psi

(*Tinnea & Brown, 1996*). In 1996, after Zone 16 had been operating for 1½ years as a GACP system (the structure and anode lead wires were electrically shorted) and 1½ years of ICCP operation, adhesion testing showed bond strengths in excess of 370 psi, the limits of the test instrument (*Tinnea & Brown, 1996*). This increase in bond strength in the early service live follows what was reported for electrochemically aged test slabs (*Covino, 1996*).

In 2004/2005 inspectors noticed significant delamination of the TS zinc in the two east arch zones of Span 8, Zones 18 and 20 (*Cramer, 2006*). In 2008, inspectors reported that 80 to 90 percent of the zinc anode on Zone 18, Pier 9, had delaminated (*Cramer & Anderson, 2009*).

Cramer & Anderson (*Cramer & Anderson, 2009*) noted that as thermal-sprayed zinc anodes age, local conditions can produce an almost infinite family of curves following the bond strength over time. The above discussion, Section 4.3.1.3, provides some background on how those local conditions can vary in ways that will impact CP current density. Over the long term, since it appears that the zinc-concrete bond degrades with CP charge passed across the interface (*Covino, 2002; Cramer & Anderson, 2009*) we would expect to encounter variation of bond strength within a single zone.

4.3.2 Visual Inspection

The condition of the zinc over the zones inspected varied considerably. Several zones exhibited good adhesion of the zinc with 100% coverage. Other zones were in poor to totally failed condition with the zinc peeling or missing over much of the surface. In Span 8, see Figure 4.7, note the configuration of Zones 17, 18, 19, and 20. Zones 17 and 19 abut at the crown of the west arch as do Zones 18 and 20 at the crown of the east arch. In the east-west direction, Zones 17 and 18 abut at the midpoint of three cross braces that connect the east and west arches, and Zones 19 and 20 do likewise on the north half of the span.

During construction, the boundaries between these abutting zones were masked using duct tape prior to application of the TS zinc coating. The zinc applicator would spray right across the duct tape masking, so the surface preparation and zinc application at abutting joints would be at least in construction terms identical, or at least as much as is possible in field work.

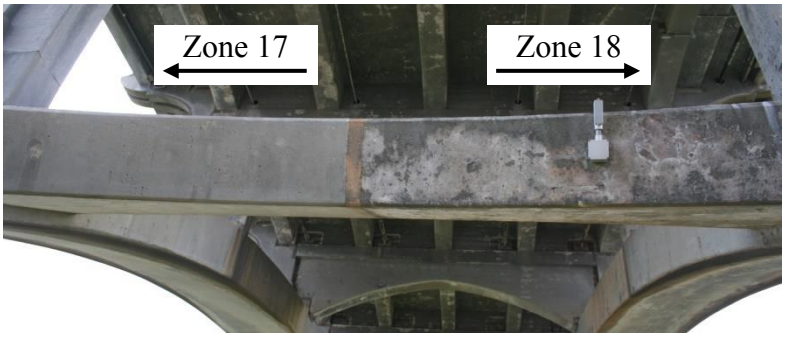

Figure 4.9: Break between Zones 17 & 18

Figure 4.9 shows a zone break which separates Zone 17 and Zone 18 on a cross brace between the east arch on the right and the west arch on the left. The zinc on the east arch, Zone 18, has failed while the zinc on the west arch, Zone 17 is still in excellent condition.

Figure 4.10 shows a zone break between Zones 18 and 20 in photographs taken in 2008 and 2011. In each figure Zone 18 is on the left. Note how much more zinc has been lost from the vertical face of Zone 20 in a time period of just three years.

Figure 4.10a: Zone 18 & 20, 2008

Figure 4.10b: Zone 18 & 20, 2011

Figure 4.11 shows an upper area on the south face of the east column of Zone 16 – Pier 9. Again note how much more zinc is missing from the concrete surface in a period of about three years.

Figure 4.11a: Zone 16 S. Face, E. Col., 2008

Figure 4.11b: Zone 16 S. Face, E. Col., 2011

This work did not include providing a definitive inventory of damaged zinc present on these zones. That said, it is clear from our visual inspection that considerably more zinc has delaminated compared to photographs obtained only three years before. These findings indicate that the integrity of the zinc-concrete bond of remaining zinc coating in Zones 16, 17, 18, 19, and 20 is likely compromised.

In addition to the zinc condition, the rectifier cabinet was also inspected. The rectifiers were all found to be unplugged and sitting piled up on the bottom of the cabinet. It is unknown if any of the rectifiers still function. Figure 4.12 shows the condition of the rectifiers at the time of inspection.

Figure 4.12: Yaquina Bridge Pier 9 Rectifiers

4.3.3 Gecor 9 Testing

Corrosion potentials and corrosion rate testing was performed at twelve total locations on the structure. Six of these locations were on a pier zone (Zone 16) while the other six were located on the east arch of Span 8 (Zone 18). Rebar potentials measured on Zone 16 ranged between -258mV and -67mV to a Cu-$CuSO_4$ reference electrode. These numbers are at the border of indicating active corrosion of steel reinforcement embedded in atmospheric exposed concrete; however the corrosion rate testing showed low corrosion risk, suggesting passive or mostly passive behavior. Zone 18 potentials ranged from -122mV to 9mV. According to NACE SP-0290, if corrosion potentials are more positive than -200mV, corrosion of the rebar is unlikely. Additionally, the corrosion rate testing returned values indicative of low corrosion risk at all Zone 18 locations. Complete results of the testing can be found in Appendix F.

4.4 EVALUATE EFFECTIVENESS OF GECOR 9

The overall effectiveness of the Gecor 9 was rated based on several factors including its performance and accuracy as an electrochemical instrument, its usability, and its durability. These factors were quantitated into a weighted scale with the instrument's performance worth 25 points, its usability worth 10 points, and its durability worth 5 points for a total of 40 possible.

4.4.1 Performance

4.4.1.1 Correlation of Readings with Observed Conditions

It is important, when testing a state-of-the-art tool, to ensure that the readings you receive while testing are at once accurate and meaningful. The Gecor 9 takes several different types of readings, and so confirming the accuracy of each, or at least verifying that the readings are within an expected range, is important practice.

Rebar corrosion potentials were the easiest to confirm. After taking readings with the Gecor, potential readings were taken using a calibrated, portable reference electrode and compared to the Gecor readings. When the reference electrode is placed on the surface of the concrete it is typically one to two inches away from the rebar. This produces a voltage that is an average of potentials occurring on the surface of the reinforcement.

As discussed above in 2.1.4.2, how much of the rebar surface is included in a corrosion potential reading depends on where the reference electrode is located, the distance between the reference electrode porous tip and the reinforcement, and the resistivity of the concrete. Figure 2.10 shows a location where rebar corrosion potential can change hundreds of millivolts when the reference electrode is moved just one foot (*Tinnea & Feuer, 1985*).

Fortunately, at Coos Bay the reinforcement potentials did not change so abruptly, but still all readings obtained were an average of values that would be observed if the reference were located a few mils above the steel surface. Corrosion potentials for embedded rebar obtained with the Gecor were found to be within 5mV of readings obtained with a calibrated reference electrode.

The Coos Bay Gecor tests were performed on zones where the zinc metalized coating had already been applied. To further review the performance of the Gecor, we ran tests in areas of Span 9 prior to the application of the thermal spray zinc coating.

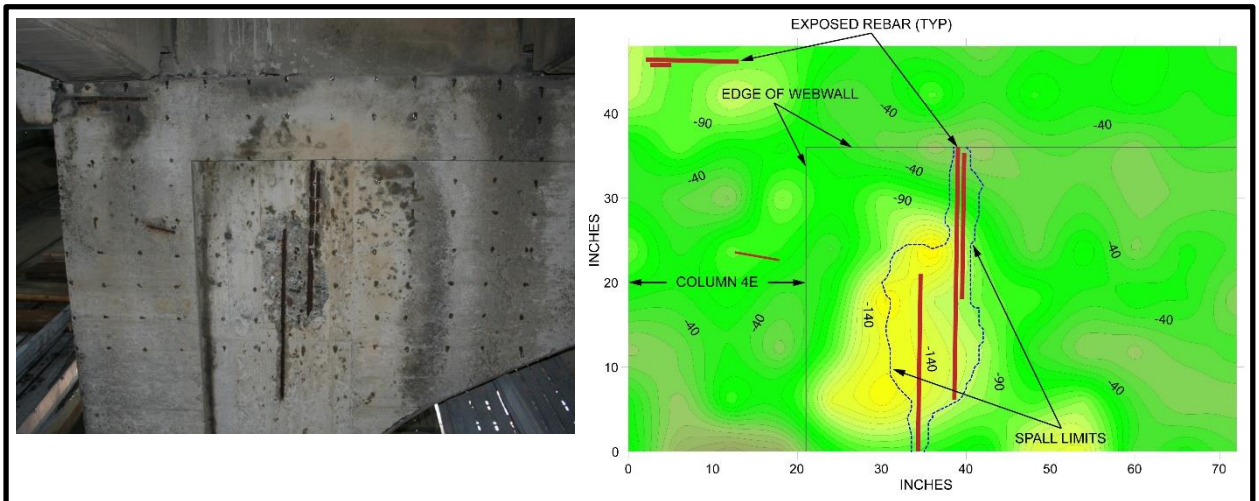

Figure 4.13: Photo & Corrosion Potential Map on Column 4E, Zone 5, Span 9, Coos Bay (Potentials mV, CSE)

On the left side of Figure 4.13, is a photograph of the area mapped. The locations where the rebar corrosion potentials were obtained appear as dark dots in the photo. The dots are the dabs of electrically conductive gel applied to the concrete surface. On right of Figure 4.13 is a contour map of equipotentials based upon the data obtained at that location. Noted on the contour map are the outline of the webwall, the limits of a concrete spall, and several corroding rebars. The data was obtained on the south face of Beam 4.

Two things of note in Figure 4.13 are the shallow concrete cover (< 0.5 inches) in the area of the exposed rebars and the surprisingly positive corrosion potentials, more electropositive than -200 mV, CSE. The corrosion of the steel reinforcement with shallow cover may be from chloride exposure, or given the age, from carbonation. We made no effort to define the cause of corrosion.

The actual rebar corrosion rate is difficult to confirm. The primary means of testing corrosion rate was to use the provided dummy cell. 15 readings are taken with the dummy cell and checked against the desired values from the manual. The Gecor manual states readings should be within 10% of the nominal result to be acceptable, and we found all of our dummy cell readings to be within that range.

A secondary means to access the corrosion rate is confirming that the readings returned are within a feasible range. Several of the readings taken early on gave largely nonsensical corrosion rates. After some examination, it was determined that the accuracy of the readings is highly dependent upon the physical stability of the electrode during testing and the presence of contaminants on the concrete surface. If the electrode moved at all during testing, or if there was remaining zinc on the surface, the corrosion rates would show extremely high readings. Further, if there was too much water in the sponge between the Gecor probe and the concrete and it

allowed bridging to the surrounding zinc, causing dramatic measurement errors and stability problems.

Returning to Span 9, Figure 4.14 shows a similar photograph and corrosion potential contour map that was also obtained on the south face of Beam 4, but at Column 4A on the east side of the beam. Note in the potential map the area of delamination shown and where the Gecor test site

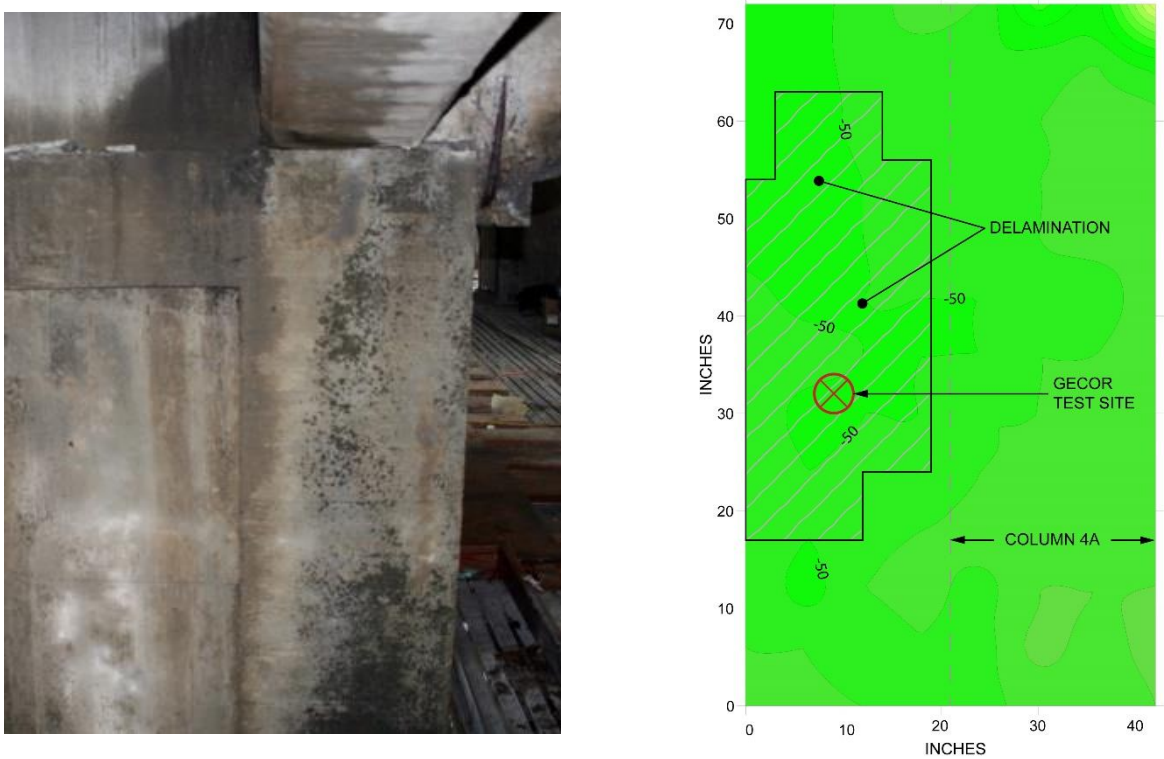

Figure 4.14: Photo & Corrosion Potential Map on Column 4A, Zone 5, Span 9, Coos Bay (Potentials mV, CSE)

was located. Also note the presence of electropositive corrosion potentials. At the test location the Gecor measured a potential of -41 mV, CSE, and a corrosion rate of 0.25 µA/cm which is indicative of low to moderate corrosion. The resistivity was measured at 9.4 kohm-cm a value that falls in the high risk category. Given the delamination, resistivity, and measured corrosion rate, it appears that early corrosion is occurring in this area. It should be noted that the cover was only one inch, so the Gecor probe was offset to try and provide the minimum distance of 5 cm between the counter electrode and the rebar.

The most difficult to confirm measurement taken by the Gecor is the PVT testing since this test is the most unique one performed by the device. At Coos Bay the zinc coating was already applied prior to conducting testing and this precluded being able to clearly locate the position of embedded reinforcement prior to removing the zinc. Where possible, we used secondary keys, like the location of a rebar bond or a test well to make estimates of the path of the rebars. Some of the Coos Bay readings may be skewed by off-center reinforcement. Also, as noted above, we clearly identified corrosion activity in areas with electropotentials more electropositive than what routinely is observed. Some of this later corrosion behavior may be a function of shallow cover and/or permeable concrete, where oxygen transport is less impeded. It is well known that rebar

potentials in water saturated concrete can be skewed to more electronegative levels than their corrosion activity would suggest.

Given the above issues at Coos Bay, we chose to verify the accuracy of the PVT test, using the first and final tests performed at the Lint Creek Bridge. By comparing the initial potentials with the results of the PVT testing, then comparing those readings to the final potential measurements and PVT results, we were able to observe a correlation between increases in PVT "protected" readings and an electropositive shift in potential. This is what is expected as the steel polarizes over time. The PVT readings were shown to have a variation in consistency if the sensor was moved during testing.

As a whole, the Gecor provided excellent consistency and accuracy during testing. The largest impediment during testing was the requirement to keep the concrete surface clear of all contaminants and to keep the sensors perfectly still during testing. We scored the Gecor a 20 out of 25 in this area.

4.4.2 Usability

4.4.2.1 Complexity

The Gecor performs a variety of advanced electrochemical tests, and as a result is quite complex to operate. The manual provided is detailed, but as it is an English translation from Spanish, is often difficult to comprehend. Likewise, the user interface of the device is inherently made more difficult due to the same translation issues. The on-site help from the manufacturer was instrumental in moving past these difficulties. Beyond the translation problems, the user interface is clunky requiring push-button function keys to the side of the screen rather than simply using a touch-screen interface.

The device is heavier and bulkier than it needs to be as it is built around PC hardware rather than more current mobile device technology and employs a NiCad battery rather than a new and lighter lithium battery. Although the case provides protection, it could be improved to make it weather tight and thereby more suitable for use in the rain without having to operate it out of a plastic bag or separately purchased weatherproof case.

4.4.2.2 Suitability to Task

For the task at hand, namely the corrosion evaluation of a large civil structure protected by impressed current cathodic protection, the Gecor is a truly remarkable device. The tests it performs are custom-tailored to this exact environment and allow for tests not available on other devices.

The suitability to task of the Gecor is excellent. However, given the interface problems, we scored the Gecor a 6 out of 10 for usability.

4.4.3 Durability

The durability of the Gecor is largely very good. During the testing, it definitely took several kicks, bumps, and short drops while still functioning as designed. The system was exposed to

rain on several occasions and appears to be largely water resistant. The cords were stepped on regularly and show no signs of significant wear or damage. The only problem encountered was with the battery which has a poor connection to the unit, and caused delays in testing due to that loss of connection several times during the inspections. The battery is also custom-built for the Gecor and therefore cannot be easily replaced.

We scored the Gecor's durability at 4 out of 5. This gives the Gecor a total rating of 30 out of a possible 40 points.

5.0 CONCLUSIONS AND RECOMMENDATIONS

5.1 CONCLUSIONS

5.1.1 CP Systems

5.1.1.1 Coos Bay Bridge

Assessing the effectiveness of CP systems on large, reinforced concrete structures is not as straight-forward as it is on marine or buried steel structures. This is due, in large part, to the high resistivity which slows down the electrochemical reactions that take place and alkalinity of concrete that can afford a return to non-corroding passive conditions as a result of the application of CP. As a result, application of low current density CP, such as ODOT employs, to steel in concrete can take over a year or more to fully polarize.

From April to June 2012, the percentage of protected zones, as identified by the Gecor PVT test, increased from approximately 30% to 48%. Unfortunately the power to the CP system was lost between June and the final inspection in September of 2012. The loss of power led to the steel depolarizing, heavily influencing the final data. However, the shift from 30% to 48% protection in less than 3 months is a good sign that the steel is passivating over time throughout the structure and that the CP system is functioning. Given what was observed in this work at Lint Creek and Yaquina Bay, the continued application of CP current to reinforcement at Coos Bay will return the reinforcement to fully passive conditions.

PVT testing of the structure indicated that across all three test dates, there was no drop in the level of protection between the 0.200 mA/SFT zones and the 0.100 mA/SFT zones. In fact the 0.100 mA/SFT zones showed slightly higher rates of passivation than the 0.200 mA/SFT zones. This is likely due to limits on sample size (18 total test points), but still indicates that a system-wide current density of 0.100 mA/SFT would likely still protect the structure and cut the present nominal required ODOT CP system operation current density in half.

The difference between constant current and constant voltage zones was also examined. The goal in this case is to identify if constant voltage rectifiers would still provide protection or if constant current rectifiers are needed. Constant voltage rectifiers, if effective, would provide a cost savings both in output and in upfront costs as constant voltage rectifiers are cheaper and typically require less maintenance than constant current rectifiers. The PVT testing data can be found in Appendix D. If you combine all tests from the three site visits and combine the results, 32% of the test locations under constant current showed protection while approximately 30% of the test locations under constant voltage showed protection. This proximity of those two numbers suggests that constant voltage rectifiers can protect the system as effectively as constant current rectifiers.

5.1.1.2 Lint Creek Bridge

The GACP system in the Lint Creek Bridge is functioning very well. The final PVT test performed in September 2012 showed that all six test locations are protected. In addition, the potential readings are all shifting more positive, indicating a return in the concrete's chemistry to

a more alkaline environment. This will help keep the steel passive and lower the current output of the anodes.

5.1.1.3 Yaquina Bay Bridge

The condition of the zinc on the Yaquina Bay Bridge varies significantly by zone. As was noted by previous citations (*Holcomb, 2002; Tinnea & Cryer, 2008*), there were rectifier malfunctions that resulted in excessive output voltage and high current output in several zones.

Excessive current output will lead to a more rapid deterioration of the zinc (*Covino, 2002*). Although there was some localized variation in damage (see Figure 4.8 a & b), the TS zinc-concrete bond for Zones 16, 18, and 20 is compromised. Given that adjacent Zones 17 and 19 show no degradation of zinc-concrete bond, we are not able to propose any other rational explanation for the zinc adhesion failure of Zones 16, 18, and 20 other than excessive rectifier output for an extended, but unknown, period of time.

The functionality of the rectifiers could not be confirmed as they were all unplugged and no power was available on site to test them.

Corrosion rate and potential testing on the bridge indicate a low corrosion risk for the steel on the bridge at this time. Since the CP system on the bridge was functioning for many years, the applied CP current drew-out chloride from the level of the reinforcement to the concrete surface. This is functionally equivalent to electrochemical chloride extraction, and it can extend the life of a structure for many years before the chloride can migrate back to the level of the steel and CP is again required.

5.1.1.4 Output Current Required for CP

For ODOT bridges, the minimum required CP current density needed to protect embedded steel depends on several factors including: pore water pH; chloride ion concentration at rebar level; the type of system; and rebar density. Bennett et al (*Bennett, 1994*), recommended the following CP current densities based on chloride content at the level of the reinforcement:

Table 5.1: CP Current as Function of Chloride Content at Steel Surface (*Bennett, 1994*)

lb Cl^-/yd^3	Cl^- Percent by Weight of Cement	CP Current Required mA/ft^2
< 1	< 0.2	0
2	0.3	0.5
5	0.8	1.1
10	1.6	1.6

The International Organization for Standardization standard ISO 12696-2012 states that typical current requirements for steel in chloride contaminated concrete range 2 to 20 mA/m² (0.19 to 1.85 mA/SFT) of steel surface and that most systems will provide full protection at current densities below 10 mA/m² (0.09 mA/SFT). To protect passive steel, what is referred to as cathodic prevention, ISO 12696-2012 says the typical current requirements range from 0.2 to 2.0 mA/m² (0.019 to 0.19 mA/SFT).

In 5.1.1.1 we suggested ODOT employ 0.1 mA/SFT as a base output for the rectifiers at Coos Bay. The conditions at Coos Bay differ from most of the other structures ODOT has protected with TS zinc coating ICCP systems, so our recommendation for Coos Bay should not be taken to be globally applied to all similar ODOT CP systems either now in operation or that will be installed in the future. Although some active corrosion is occurring, a significant portion of the Coos Bay Bridge reinforcement is passive. Hence, the application of CP at Coos Bay is in part cathodic prevention, and lower current densities are therefore appropriate.

This present work did not include monitoring of the galvanic anodes installed at Lint Creek. Based on previous work (*Ball & Whitmore, 2009*), it is reasonable to expect current output from the embedded galvanic anodes to directly follow temperature changes, with output rising and falling with temperature increased and drops. It is also reasonable to expect that the average output of the embedded anodes diminishes with time (*Ball & Whitmore, 2009*, *Dugarte & Sagüés, 2014*). The work did show that with time increasing indications of the steel reinforcement returning to passive behavior.

As noted in 2.2.2, with time the application of CP will effect migration of chloride ions from the rebar surface and concurrently increase the pH of the porewater at steel-concrete interface. With an appropriate applied CP current density, this leads in time to the steel returning to passive behavior (see 2.2.5). In 2.4.1 this over time changing of the environment surrounding the rebar to one that supports passivated behavior speaks to the possibility of operating CP systems on an intermittent basis. What was observed during this work at Yaquina Bay showed that when CP systems were not providing protective current for extended periods, the reinforcing steel continued to show passive behavior and did not promptly return to unacceptable levels of corrosion activity.

5.1.2 Gecor 9

As stated above in 4.5, we scored the Gecor according to accuracy and precision, usability, and durability. The Gecor earned a 30 out of 40 possible points, or to qualify, it is a good device that performs a variety of unique tests, but the poor execution in the user interface and the translation issues in the user interface and manual made for a more difficult experience than it needed to be.

Considering that the sensor needs to be held perfectly still for often up to 15 minutes, the sensor needs a more effective means of securing it to the structure than eye bolts and bungee cords.

The Gecor 9 is not an instrument for a technician level person to take to the field and bring back data for later review by someone well versed in the corrosion of steel in concrete. There are simply too many ways errors can be introduced to employ this device without someone technically competent immediately available on site to review the data and observations.

5.2 RECOMMENDATIONS

5.2.1 CP System Operation

5.2.1.1 Coos Bay Bridge

While the CP system is functioning and providing some protection, some changes should be made to the system in order to extend the system's life and better protect the structure.

1. The testing performed indicates that constant voltage rectifiers are as effective as constant current at this location. However, long term protection data of constant current versus constant voltage would be worthwhile to obtain. Therefore we recommend changing six (6) of the constant current zones to constant voltage and leaving another six (6) as constant current to monitor the long term differences. When changing the rectifiers to constant voltage, set the voltage to the level required to reach the current density outlined in number 2 below. Then wait a minimum of two (2) days and reset the voltage so to meet that current density. Resetting of the constant voltage would best be performed in either the spring or fall when the structure temperature is above 45 °F and is expected to remain so for several days. Mid to late summer should be avoided as the concrete will be at its driest.

2. Current densities for all zones should be set to 0.100mA/SFT. The 0.100mA/SFT density was shown to be as effective as the 0.200mA/SFT zones at providing protection and will effectively double the life of the system.

3. After items 1 and 2 are completed, a follow-up inspection should be performed including PVT testing of the 21 zones. This inspection should occur approximately three (3) years after final adjustment of the CP system to allow time for polarization of the steel to the new current densities.

5.2.1.2 Lint Creek Bridge

The CP system on the Lint Creek Bridge is functioning well with no deficiencies. We recommend that the system be inspected again within five (5) years to ensure it is continuing to provide protection to the beams.

5.2.1.3 Yaquina Bay Bridge

While the CP system is not active on the Yaquina Bay Bridge, the bridge itself is in good condition and testing indicates that the reinforcement is not actively corroding. It is likely to take several years for the chloride to return to the level of the reinforcement at most locations, meaning a replacement of the CP system would not be needed until that time. Tinnea & Associates recommends performing a corrosion condition inspection including sounding, potential mapping, and corrosion rate testing every five (5) years.

5.2.1.4 CP Rectifiers

At both Yaquina Bay and Coos Bay there were problems with the "rectifiers" employed to provide CP current. We are also aware that there have been rectifier problems at Cape Creek. As

engineers working in the area of providing cathodic protection to structures in profoundly diverse environments, we would not call these units CP rectifiers. They are laboratory DC power supplies that were not designed to provide continuous power to bridge elements even from boxes that provide a controlled environment, like those at Coos Bay, let alone a box that is not environmentally controlled such as Yaquina Bay.

At the north approach of Yaquina Bay, a commercial CP rectifier was installed to provide power to the carbon paint CP system. That unit operated well for over 25 years. We recommend that in the future when ODOT encounters failed rectifiers, they give very serious consideration to replacing the failed lab power supplies or in-house designed equipment with field-proven rectifiers designed to provide CP power to multi-zone reinforced concrete structures. There are a number of commercial manufacturers of such specialized rectifiers.

5.2.2 Gecor 9

The Gecor 9 is an excellent tool for performing a variety of electrochemical tests. Like any advanced tool, it should be operated by someone with a strong understanding of electrochemistry – specifically of corrosion in reinforced concrete. Given the often awkward translation, technicality of the readings, and the fickleness of the sensor to movement and contaminants, the person using the device should be able to understand when the device is giving accurate results and when they are nonsensical. This is not a tool for technician-level staff, but for more advanced personnel that understand corrosion rates, potential readings, and passivity. Assuming such ODOT staff has time available to perform testing, or be available on-site during testing, we would not hesitate to recommend the device to staff.

6.0 REFERENCES

ACI 222R, *Protection of Metals in Concrete Against Corrosion*, ACI International, Farmington Hills, MI, 41 pp., (2010).

ASTM C876-09, *Standard Test Method for Corrosion Potential of Uncoated Reinforcing Steel in Concrete*, ASTM International West Conshohocken, PA, 7 pp., (2009).

C. Andrade, I. Marinez, and X. R. Nóvoa, *Passivity Verification Technique Applied to Cathodically Protected Structures*, 15th International Corrosion Congress Proceedings, Granada Spain, 8 pp. (2002).

C. Andrade, R. Polder, and M. Basheer, *Non-Destructive Methods to Measure Ion Migration*, Chapter 5 of Non-Destructive Evaluation of Penetrability and Thickness of Concrete Cover, RILEM TC 189-NEC, RILEM, Bagneux, France, 22 pp. (2007).

D.M. Bastidas, J. A. González, S. Feliu, A. Cobo, and J.M. Miranda, *A Qualitative Study of Concrete-Embedded Steel Corrosion Using Potentiostatic Pulses*, Corrosion Journal, Vol. 63, No. 12, NACE International, Houston, TX, pp. 1094-1100, (2007).

J.C. Ball and D.W. Whitmore, *Galvanic Protection for Reinforced Concrete Bridge Structures; Case Studies and Performance Assessment*, Australasian Corrosion Association, Coffs Harbour, AU, 8 pp. (2009).

J.P. Broomfield and J.S. Tinnea., *Cathodic Protection of Reinforced Concrete Bridge Components*, SHRP-C/UWP-92-618, Strategic Highway Research Program, National Research Council, Washington, DC, 84 pp., (1992).

S.J. Bullard, S. Cramer, and B. Covino, *Effectiveness of Cathodic Protection*, Final Report, SPR 345, Oregon Department of Transportation, Salem OR, and Federal Highway Administration, Washington D.C., 27 pp. (2009).

K.C. Clear, *Time to Corrosion of Reinforcing Steel in Concrete Slabs*, FHWA-RD-76-70, Federal Highway Administration, Washington, DC, pp., (1987).

B.S. Covino Jr., S.J. Bullard, G.R. Holcomb, S.D. Cramer, G.E. McGill, and C.B. Cryer, *Bond Strength of Electrochemically-Aged Arc-Sprayed Zinc Coatings on Concrete*, Paper No. 96308, CORROSION/96, NACE International, Houston, TX, 17 pp. (1996).

B.S. Covino Jr., S.J. Bullard, S.D. Cramer, G.R. Holcomb, G.E. McGill, and C.B. Cryer, *Interfacial Chemistry of Zinc Anodes for Reinforced Concrete Structures*, Paper No. 97233, CORROSION/97, NACE International, Houston, TX, 20 pp. (1997a).

B.S. Covino Jr., S.J. Bullard, G.R. Holcomb, S.D Cramer, G.E. McGill, and C.B. Cryer, *Bond Strength of Electrochemically Aged Arc-Sprayed Zinc Coatings on Concrete*, Corrosion Journal, Vol. 63, No. 12, NACE International, Houston, TX, pp. 399-411, (1997b).

B.S. Covino Jr., S.D. Cramer, S.J. Bullard, G.R. Holcomb, J.H. Russell, W.K. Collins, H.M. Laylor, and C.B. Cryer, *Performance of Zinc Anodes for Cathodic Protection of Reinforced Concrete Bridges*, Final Report, SPR 364, Oregon Department of Transportation, Salem OR, and Federal Highway Administration, Washington D.C., 136 pp., (2002).

S.D. Cramer, S.J. Bullard, B.S. Covino Jr., G.R. Holcomb, and J.H. Russell, *Carbon Paint Anode for Reinforced Concrete Bridges in Coastal Environments*, Paper No. 02265, CORROSION/2002, NACE International, Houston, TX, 16 pp. (2002).

S.D. Cramer, B.S. Covino, G.R. Holcomb, M. Ziomek-Moroz, and J. Tinnea, *Conventions and Definitions in Corrosion and Oxidation*, ASM Handbook, Vol. 13A, ASM International, Materials Park, OH, p. 1006, (2003)

S.D. Cramer, S.J. Bullard, B.S. Covino, M. Ziomek-Moroz, G.R. Holcomb, and J. Tinnea, *Intermittent Application of Cathodic Protection*, Interim Report, SPR 317, Oregon Department of Transportation, Salem OR, and Federal Highway Administration, Washington D.C., 74 pp., (2005).

S.D. Cramer, S.J. Bullard, and B.S. Covino Jr., *Zinc Anode Delamination of Arches Section of Yaquina Bay Bridge*, Interim Report to Bridge Section, Oregon Department of Transportation, Salem, OR, (2006).

S.D. Cramer and M.D. Anderson, *Zinc Anode Aging on the Arches and south Approach Sections of the Yaquina Bay Bridge – May 2007*, submitted to Bridge Preservation Section as part of Contract No. EA 08BRPG3/201 P51 574, 66 pp. (2009).

M.J. Dugarte and A.A. Sagüés, *Sacrificial Point Anodes for Cathodic Prevention of Reinforcing Steel in Concrete Repairs: Part 1 – Polarization Behavior,* Corrosion Journal, Vol. 70, No. 3, NACE International, Houston, TX, pp. 303-317, (2014).

E. Escalante, S. Ito, and M. Cohen, *Measuring the Corrosion Rate of Reinforcing Steel in Concrete*, NBS IR 80-2012, National Bureau of Standards, Washington, DC (1980).

E. Escalante, M. Cohen, and A.H. Kahn, *Measuring the Corrosion Rate of Reinforcing Steel in Concrete*, NBSIR 84-2853, U.S. Department of Commerce, (1984).

E. Escalante, *Effectiveness of Potential Measurements for Estimating Corrosion of Steel in Concrete*, in Corrosion of Reinforcement in Concrete, eds. C.L. Page, K.W.J. Treadaway, P.B. Bamforth, Elsevier Applied Science, London, UK, pp. 281-292, (1990).

S. Feliu, J.A. González, M.L. Escudero, S. Feliu Jr., and M.C. Andrade, *Possibilities of the Guard Ring for Electrical Signal Confinement in the Polarization Measurements of Reinforcements*, Corrosion Journal, Vol. 46, No. 12, NACE International, Houston, TX, pp. 1015-1020, (1990a).

S. Feliu, J.A. González, S. Feliu Jr., and M.C. Andrade, *Confinement of the Electrical Signal for In Situ Measurement of Polarization Resistance in Reinforced Concrete*, ACI Materials Journal, Vol. 87, No. 5, ACI International, Farmington Hills, MI, pp. 457-460, (1990b).

S. Feliu, J.A. González, and M.C. Andrade, *Multiple-Electrode Method for Estimating the Polarization Resistance in Large Structures*, Journal of Applied Electrochemistry, Vol. 26, pp. 305-309 (1996).

V. Feliu, J.A. González, C. Andrade, and S. Feliu, *Equivalent Circuit for Modelling the Steel-Concrete Interface, I. Experimental Evidence and Theoretical Predictions*, Corrosion Science, Vol. 40, No. 6, pp. 975-993, (1998).

F.W. Fink, *Corrosion of Metals in Concrete*, US Dept. of Interior, Office of Saline Water, Report No. 46, (1960).

G.K. Glass, A.M. Hassanein, and N.R. Buenfeld, *Cathodic Protection Afforded by an Intermittent Current Applied to Reinforced Concrete*, Corrosion Science, Vol. 43 pp. 1111-1131, (2001).

G. Glass, J. Taylor, A. Roberts, and N. Davison, *The Protective Effects of Electrochemical Treatment in Reinforced Concrete*, Paper No. 03291, CORROSION/2003, NACE International, Houston, TX, 10 pp. (2003).

G.R. Holcomb, B.S. Covino Jr., S.D. Cramer, J.H. Russell, S.J. Bullard, W.K. Collins, J.E. Bennett, S.M. Soltesz, and H.M. Laylor, *Humectants to Augment Current from Metallized Zinc Cathodic Protection Systems on Concrete*, Final Report, SPR 384, Oregon Department of Transportation, Salem OR, and Federal Highway Administration, Washington D.C., 131 pp., (2002).

D.G. John and D.A. Eden, *Corrosion Measurements on Reinforcing Steel and Monitoring of Concrete Structures*, Paper No. 87137, CORROSION/87, NACE International, Houston, TX, (1987).

H.M Laylor, *Soffit Cathodic Protection System in a Coastal Environment*, Final Report, Demonstration Project No. 923, DTFH71-83-923-05, Oregon Department of Transportation, Salem OR, and Federal Highway Administration, Washington D.C., 39 pp., (1989).

I. Martinez, C. Andrade, O. Vennesland, U. Evensen, R.B. Polder, and J. Leggedor, *Efficiency Control of Cathodic Protection Measured Using Passivation Verification Technique in Different Concrete Structures*, Corrosion Journal, Vol. 63, No. 9, NACE International, Houston, TX, pp. 880-892, (2007).

I. Martinez and C. Andrade, *Application of EIS to Cathodically Protected Steel: Tests in Sodium Chloride Solution and in Chloride Contaminated Concrete*, Corrosion Science, Vol. 50 pp. 2948-2958, (2008).

D. Linden, and T.B. Reddy, Handbook of Batteries, 3rd Ed., McGraw-Hill, New York, NY, (2011).

NACE/ASTM G193-12d, *Standard Terminology and Acronyms Relating to Corrosion*, ASTM International West Conshohocken, PA, and NACE International, Houston, TX, 20 pp., (2013).

NACE SP0290-07, *Impressed Current Cathodic Protection of Reinforcing Steel in Atmospherically Exposed Concrete Structures*, NACE International, Houston, TX, 15 pp., (2007).

NACE SP0308-08, *Inspection Methods for Corrosion Evaluation of Conventionally Reinforced Concrete Structures*, NACE International, Houston, TX, 24 pp., (2008).

J. Newman, *Resistance for Flow of Current to a Disk, Journal of the Electrochemical So*ciety, Vol. 107, pp. 502-502, (1996)

ODOT, *Yaquina Bay Bridge Cathodic Protection*, Bridge No. 18202, Drawing No. 48336, Oregon Department of Transportation, Salem, OR, (1991).

A.A. Sagüés, S.C. Kranc, and E.I. Moreno, *Cyclic Polarization Resistance Measurements of Concrete Reinforcing Steel with Constant Phase Angle Element Charge Storage Behavior*, Paper No. 97280, CORROSION/97, NACE International, Houston, TX, 16 pp., (1997).

M. Stern and A.L. Geary, *Electrochemical Polarization I. A Theoretical Analysis of the Shape of Polarization Curves*, Journal of the Electrochemical Society, Vol. 104, No. 1, pp. 56-63, (1957).

X. Shi, J.D. Cross, L. Ewan, Y. Liu, K. Fortune, *Replacing Thermal Sprayed Zinc Anodes on Cathodically Protected Steel Reinforced Concrete Bridges*, Final Report, SPR 682, Oregon Department of Transportation, Salem OR, and Federal Highway Administration, Washington D.C., 201 pp., (2011).

J.S. Tinnea & N.J. Feuer, *Evaluation of Structural Fatigue and Reinforcement Corrosion Interrelationships Using Close Grid Computer Generated Equipotential Mapping*, Paper No. 85259, CORROSION/85, NACE International, Houston, TX, 29 pp., (1985).

J.S. Tinnea, *Evaluation of Bridge Deck Rehabilitation Strategies*, Paper No. 91121, CORROSION/91, NACE International, Houston, TX, 22 pp., (1991).

J.S. Tinnea & R.P. Brown, *Evaluation of the Performance of Sprayed Zinc Anodes for Protection Reinforcing Bar*, ILZRO Project No. ZC-2-1, International Lead Zinc Research Organization, Research Triangle Park, NC, 76 pp., (1996).

J. Tinnea, *Field Performance of Sprayed Zinc Anodes in Controlling Corrosion of Steel Reinforced Concrete*, Paper No. 98510, CORROSION/98, NACE International, Houston, TX, 8 pp., (1998).

J.S. Tinnea, *Localized Corrosion Failure of Steel Reinforcement in Concrete: Field Examples of the Problem,* Proceedings of 15th International Corrosion Council, Granada, Spain, 8 pp. (2002).

J. Tinnea, *Electrochemical Techniques: Cathodic Protection, Chloride Extraction, and Realkylization*, ASM Handbook, Vol. 13C, ASM International, Materials Park, OH, p 387 (2006)

J.S. Tinnea and C.B. Cryer, *Corrosion Control of Pacific Coast Reinforced Concrete Structures: A Summary of 25 Year Experience*, 1st International Conference on Construction Heritage in Coastal and Marine Environments, Lisbon, Portugal, 16 pp., (2008).

J. Tinnea, *Corrosion Testing in Concrete: You Need an Array of Procedures*, Corrosion & Prevention Conference Opening Plenary Lecture, Australasian Corrosion Association, Brisbane, AU, 17 pp. (2013).

F. Wenner, *A Method of Measuring Earth Resistivity*, US Bureau of Standards Publication No. 258, pp. 469-478, (1916).